Graduate School ETD Form 9
(Revised 12/07)

PURDUE UNIVERSITY
GRADUATE SCHOOL
Thesis/Dissertation Acceptance

This is to certify that the thesis/dissertation prepared

By Samuel Assegie

Entitled Efficient and Secure Image and Video Processing and Transmission in Wireless Sensor Networks

For the degree of Master of Science in Electrical and Computer Engineering

Is approved by the final examining committee:

Chair
Brian King

Paul Salama

Maher Rizkalla

To the best of my knowledge and as understood by the student in the *Research Integrity and Copyright Disclaimer (Graduate School Form 20)*, this thesis/dissertation adheres to the provisions of Purdue University's "Policy on Integrity in Research" and the use of copyrighted material.

Approved by Major Professor(s): Brian King

Approved by: Brian King 07/27/2010
Head of the Graduate Program Date

Graduate School Form 20
(Revised 1/10)

PURDUE UNIVERSITY
GRADUATE SCHOOL

Research Integrity and Copyright Disclaimer

Title of Thesis/Dissertation:

Efficient and Secure Image and Video Processing and Transmission in Wireless Sensor Networks

For the degree of Master of Science in Electrical and Computer Engineering

I certify that in the preparation of this thesis, I have observed the provisions of *Purdue University Teaching, Research, and Outreach Policy on Research Misconduct (VIII.3.1)*, October 1, 2008.*

Further, I certify that this work is free of plagiarism and all materials appearing in this thesis/dissertation have been properly quoted and attributed.

I certify that all copyrighted material incorporated into this thesis/dissertation is in compliance with the United States' copyright law and that I have received written permission from the copyright owners for my use of their work, which is beyond the scope of the law. I agree to indemnify and save harmless Purdue University from any and all claims that may be asserted or that may arise from any copyright violation.

Samuel Assegie

Printed Name and Signature of Candidate

07/09/2010

Date (month/day/year)

*Located at http://www.purdue.edu/policies/pages/teach_res_outreach/viii_3_1.html

EFFICIENT AND SECURE IMAGE AND VIDEO PROCESSING AND TRANSMISSION IN WIRELESS SENSOR NETWORKS

A Thesis

Submitted to the Faculty

of

Purdue University

by

Samuel Assegie

In Partial Fulfillment of the

Requirements for the Degree

of

Master of Science in Electrical and Computer Engineering

August 2010

Purdue University

Indianapolis, Indiana

To my family.

ACKNOWLEDGMENTS

Foremost, I would like to express my sincere gratitude to my advisor Prof. Brian King for his continuous support, patience, motivation and immense knowledge during my graduate studies. His guidance helped me in all the time of research and writing of this thesis. I could not have imagined having a better advisor and mentor.

I would like to express my sincere gratitude to Prof. Paul Salama, for his support in my studies, providing me with research ideas and working with me closely in solving the problems.

I would like to thank Prof. Dongsoo (Stephen) Kim for his support in my research and being part of my thesis committee.

I would also like to thank Prof. Lauren Christopher and Prof. Maher Rizkalla for being part of my thesis defense committee and their positive feedback which helped me to make my thesis better. I also like to thank Ms. Valerie Lim Diemer for her help during my studies. I am grateful to all the professors in Electrical and Computer Engineering Department for their excellent teaching.

Most importantly, none of this would have been possible without the love and support of my family.

Finally, I appreciate the financial support from Electrical and Computer Engineering Department that funded my research and studies.

TABLE OF CONTENTS

Page

LIST OF TABLES vii

LIST OF FIGURES viii

ABSTRACT x

1 INTRODUCTION 1

2 BACKGROUND MATERIAL 4

2.1 Image Compression - Using Wavelets 4

2.1.1 Image/Video Compression 4

2.1.2 Wavelet Coding 5

2.2 Background Subtraction Method for Detecting Foreground Objects 7

2.2.1 Background Model - Estimating Good Background 7

2.2.2 The Most Common Approaches of Background Generation . 8

2.3 Security 10

2.3.1 Cryptography 10

2.4 Multimedia Security 12

2.4.1 Image/Video Encryption Scheme 12

2.5 Selective Encryption 13

3 SELECTIVE ENCRYPTION 14

3.1 Introduction 14

3.2 Wavelet Based Compression Techniques 15

3.3 Prior Work on Selective Encryption 17

4 ATTACKING WAVELET TREE SHUFFLING ENCRYPTION SCHEME 20

4.1 A Generic Framework of a Wavelet Tree Shuffling Encryption Scheme 20

4.2 Attacking a Wavelet Tree Shuffling Encryption Scheme 22

5 DESIGN MODEL 27

Page

5.1 Introduction - Design Summary 27
5.2 Design Goal 27
5.3 Where Does the Power Go? 29
5.4 Energy/Power Analysis of Sensor Nodes 31
5.4.1 In-Sensor (Node Level) Energy Optimization 31
5.4.2 Network-Wide Energy Optimization 32
5.5 System Model 32
5.6 Network Assumption 32
5.7 Node Power Consumption Model 33
5.8 Our First Design 34
6 ENCODER 36
6.1 Introduction 36
6.1.1 Principles of Image Compression 36
6.1.2 Classification of Compression Technique 36
6.1.3 Model/Framework of General Image Compression Method . 37
6.1.4 Wavelets for Image Compression 39
6.2 Haar Wavelet Technique 41
6.2.1 Haar Example 41
6.2.2 Filter Banks 42
6.2.3 Image Thresholding 42
6.2.4 Procedures and Experimental Results 44
6.2.5 Energy Efficient Local Processing Using DWT 45
6.3 Background Subtraction Method for Image Compression 51
6.3.1 Background Model - Estimating Good Background 52
6.3.2 The Most Common Approaches of Background Modeling . . 52
6.3.3 Foreground Processing 52
6.3.4 Improving the Run Length Encoder 53

Page

6.4 Exploiting Data Correlation Between Neighborhood Sensors for Energy Efficient Data Transmission in WMSN 55
6.4.1 Block Matching Algorithm 57
6.4.2 Transmission of Data After Receiving Codebook: Encoder Side 57
6.4.3 The Overall Encoding Process 61
7 IMAGE QUALITY ASSESSMENT BY BASE STATION 65
7.1 Introduction 65
7.2 Image Quality Assessment Tools 66
7.3 Reduced-Reference (RR) QA Methods, Our Approach (Technique) . 68
7.3.1 Thumbnail 69
7.3.2 Evaluating Thumbnail Image Quality 69
7.4 Statistical Test 74
7.4.1 Mean Test 75
7.4.2 Variance Test 76
7.5 Applying Three Metrics for Quality Assessment 78
8 DECODER 85
8.1 Decoding Packets and Coordinating Sensor Operation 85
8.1.1 Decoding Packets Received from the Sensor: 85
8.1.2 Block Matching Algorithm (BMA) 87
8.1.3 Checking Quality of the Reconstructed Image 89
9 Conclusion and Future Work 92
LIST OF REFERENCES 94

LIST OF TABLES

Table		Page
4.1	Relationship between no. of decomp. and no. of trees for an image of size 256×256	24
6.1	Computation cost, DWT (Haar filter)	47
6.2	Communication Cost, DWT (Haar Filter)	48
6.3	Simulation result, DWT (Haar filter, $L = 2$) with global and level dependent threshold	51
6.4	Encoding foreground image based on 10 neighboring images	55
6.5	Simulation Result: Number of matched blocks between two frames, with different threshold	64
7.1	PSNR value of original image vs. thumbnail image	74
7.2	Codebook results on traffic.avi video	81
7.3	Estimating retransmission requests by base station	82
7.4	Wavelet transform-2 levels of decomposition	83
7.5	Foreground - RLE with threshold (based on 10 images near background) 240×320 image (300 blocks)	84
7.6	RLE with threshold assessing by using only the variance test	84

LIST OF FIGURES

Figure		Page
2.1	Encryption and decryption of a cipher	11
3.1	The relations between wavelet coefficients in different subbands as quad-trees as illustrated in [69]. LL1 is the low-low coefficients (that is, low pass filtered in the vertical, and low pass filtered in the horizontal). LH1,HL1,HH1 are defined similarly.	16
4.1	Encrypting by shuffling wavelet trees	21
4.2	Original image	25
4.3	Shuffled image where $L = 3$	25
4.4	Shuffled image where $L = 4$	25
4.5	Shuffled image where $L = 5$	25
5.1	Sensor operation flowchart	30
5.2	Averaging and differencing to find Haar vectors	31
5.3	WMSN with 7 sensors and a single sink	33
5.4	A fist design of our encoder	35
6.1	A model for lossy image encoder	38
6.2	Wavelet decomposition of Lena (512×512, $L = 3$)	40
6.3	Computation vs. communication cost, DWT(s = 1,2,3)	50
6.4	Run length encoding, with different divisor (threshold)	56
6.5	Overlap between proximate sensor measurement	58
6.6	Reference image vs. frame with threshold = 0	60
6.7	Frame with threshold = 3 vs. frame with threshold = 9	61
6.8	Frame with threshold = 0 vs. frame with threshold = 3	61
6.9	Frame with threshold = 9 vs. frame with threshold = 0	62
6.10	Frame with threshold = 3 vs. frame with threshold = 9	62
6.11	Encoding System	63

Figure Page

7.1 Comparison of image similarity metrics among MSE, PSNR and SSIM 67

7.2 256 × 256 8-bit grayscale girls image with mean thumb image based on 4 × 4 blocking. 70

7.3 PSNR: Original-reconstructed vs. thumb version of Orig-rec 71

7.4 Image: Bicycle and its thumbnail version 72

7.5 Image: Girls and its thumbnail version 73

7.6 Image: Bicycle modified and its thumbnail version 73

8.1 Decoder design 86

8.2 Block is moved to all vertical, horizontal, left and right displacements in the search area (R from all sides of the macro block) until a match is found with in the given threshold (matching is based on mean absolute difference). 89

ABSTRACT

Assegie, Samuel. M.S.E.C.E., Purdue University, August 2010. Efficient and Secure Image and Video Processing and Transmission in Wireless Sensor Networks . Major Professor: Brian King.

Sensor nodes forming a network and using wireless communications are highly useful in a variety of applications including battle field (military) surveillance, building security, medical and health services, environmental monitoring in harsh conditions, for scientific investigations on other planets, etc. But these wireless sensors are resource constricted: limited power supply, bandwidth for communication, processing speed, and memory space. One possible way of achieve maximum utilization of those constrained resource is applying signal processing and compressing the sensor readings. Usually, processing data consumes much less power than transmitting data in wireless medium, so it is effective to apply data compression by trading computation for communication before transmitting data for reducing total power consumption by a sensor node. However the existing state of the art compression algorithms are not suitable for wireless sensor nodes due to their limited resource. Therefore there is a need to design signal processing (compression) algorithms considering the resource constraint of wireless sensors. In our work, we designed a lightweight codec system aiming surveillance as a target application. In designing the codec system, we have proposed new design ideas and also tweak the existing encoding algorithms to fit the target application. Also during data transmission among sensors and between sensors and base station, the data has to be secured. We have addressed some security issues by assessing the security of wavelet tree shuffling as the only security mechanism.

1. INTRODUCTION

Recent technological advancements have enabled the deployment of small, inexpensive, low-power, distributed devices, which are capable of performing local processing and wireless communication. Such nodes are called *sensor nodes*. Regardless of the flexibility and advantages offered by wireless sensors (compared to wire); each sensor node is capable of performing only a limited amount of processing. Sensor nodes are typically characterized by limited power supplies, low bandwidth, small memory sizes and limited energy. However by utilizing a large number of nodes sensor nodes can provide a significant amount of information about the physical environment. A sensor network can be described as a collection of large number of sensor nodes, which are densely deployed either inside the phenomenon or very close to it and coordinate to perform some specific action. Unlike traditional networks, sensor networks depend on dense deployment and coordination to carry out their tasks and transmit the sensed information to a central system.

A centralized system would mean that some of the sensors would need to communicate over long distances, which leads to even more energy depletion. Hence, it would be a good idea to process locally as much information as possible in order to minimize the total number of bits transmitted. In most cases, the environment to be monitored does not have an existing infrastructure for either energy or communication, so it becomes necessary for sensor nodes to survive on small, finite sources of energy and communicate through a wireless communication channel. With high energy cost for wireless communication it is infeasible to transmit the sensed data in a clear. Application algorithms have to be designed to reduce data size (communication cost). For energy efficient operation of sensors both the network protocol and signal processing algorithms has to be optimized.

The resource constraint in power, memory size, energy and bandwidth leads to a very demanding environment to secure the information transmitted to the central system or the data communicated between sensors. Public-key cryptography is too expensive to be usable, and even fast symmetric-key ciphers must be used carefully [52]. Communication bandwidth is extremely precious: each bit transmitted consumes about as much power as executing $800 - 1000$ instructions [51] and as a consequence, any message expansion caused by security mechanisms comes at significant cost.

In our work, we have focused more on optimizing/devising signal processing algorithms to be used on these resource constrained multimedia sensors. This thesis is organized as follows:

In Chapter 2, we provide background material in image and video processing, some of the most common encoding techniques for light weight encoding, background on security and wireless sensor networks.

In Chapter 3, we discuss some security protocols and tools used to encrypt the data during transmission towards the base station and we have reviewed some previous works on selective encryption.

In Chapter 4, We attacked a work by Kwon et. al. and showed the insecurity (design flaw) of wavelet tree shuffling when used as the only security mechanism in multimedia encryption.

In Chapter 5, we discus about our design model, the overall network assumption, system model and node power consumption model.

In Chapter 6, we discuss the wavelet and background subtraction based image coding schemes and provide some techniques to optimize the encoding algorithms for light weight processing. Also we have addressed some techniques to compress the signal efficiently by sharing some of the computationally intensive work with the decoder and communicate using the backward channel.

In Chapter 7, we propose some techniques to evaluate the quality of reconstructed image at the decoder side with out having the original image. We used some partial

information about the original image sent along with the data as a side information to compare the quality of the reconstructed image.

In Chapter 8, we describe the over all design of the decoder and the decoding process. We also propose a block matching algorithm technique to predict position vectors and give the information back to the encoder to reduce computation.

In Chapter 9 we conclude and discuss future work.

2. BACKGROUND MATERIAL

2.1 Image Compression - Using Wavelets

Images require substantial storage and transmission resources, thus image compression is advantageous to reduce these requirements. This chapter covers some background of wavelet analysis, data compression and how wavelets have been and can be used for image compression.

2.1.1 Image/Video Compression

Image data by its nature is multidimensional and tends to take up significant space (storage), computations (during its processing, such as in compression and encryption) and transmission time and bandwidth. For example, two hours of video, in HDTV resolution

$$2 \times 60 \times 60 \times 30 \times 1920 \times 1080 \times 3 = 1.22\text{terabytes}.$$

There are several constraints for transmitting the multimedia data in raw format, such as transmission time and costs (ISPs charge per data amount, whereas phone companies charge per time unit), limited hardware resources such as memory, CPU etc (PDA, Cell phone, wireless sensors etc). Compressing an image is significantly different than compressing raw data. Thus, general purpose compression programs are not optimal when they are applied to compress a multimedia data since multimedia data possess statistical properties which can be exploited by encoders specifically designed for them. Also, the human visual system does not rely on quantitative analysis of individual pixel values when interpreting an image - an observer searches for distinct features and mentally combines them into recognizable groupings. In this

process certain information is relatively less important than other and some of the finer details in the image can be sacrificed to save more bandwidth and storage space.

The fundamental task of image compression is to reduce the amount of data required to represent an image. This is done by transforming and removing image data redundancies mathematically; this is accomplished by transforming the data to a statistically uncorrelated set. The two major categories of compression algorithms are:

Lossless compression algorithms In this case the original data is reconstructed perfectly. Theoretical limits exist concerning maximal compression performance. Practical compression ratios are less than $10:1$ (for still images).

Lossy compression algorithms In this case the the decompression results in an approximation of the original image. Maximal compression rate is a function of reconstruction quality, and practical compression ratios can be greater than $10:1$ (for still images).

2.1.2 Wavelet Coding

A mathematical transformation is applied to signals to obtain further information from that signal that is not readily available in the raw signal. Most of the signals in practice are *TIME-DOMAIN* signals in their raw format. That is, whatever that signal is measured it is a function of time. When we plot a *time-domain* signal, we obtain a *time-amplitude* representation of the signal. For most signal processing related applications, this representation is not always the best representation of the signal. In many cases, the most distinguished information is hidden in the frequency content of the signal. The *frequency spectrum* of a signal is basically the frequency components (spectral components) of that signal and it shows what frequencies exist in the signal.

We can measure the frequency content of a signal by applying mathematical transform to the time-domain signal. Some of the mathematical transforms that

are used Fourier Transform (FT), Discrete Cosine Transform (DCT), Radon Transform, Wavelet Transform, etc. If the Fourier transform of a signal in the time domain is taken, we obtain the frequency-amplitude representation of that signal.

The *frequency* information of a signal is needed, because often, information that cannot be readily seen in the *time-domain* can be seen in the *frequency domain*.

In electrical engineering, the Fourier transform is one of the most common and widely used mathematical transformation techniques to convert the signal from time domain to frequency domain.

For any periodic signal $f(t)$, its Fourier transform is:

$$F(\omega) = \int_{-\infty}^{\infty} f(t)e^{-j\omega t}dt$$

The Fourier transform gives the frequency information of the signal, which means that it provides how much of each frequency component exists in the signal, but it does not tell us when, in time, these frequency components exist. Signals whose frequency content do not change in time are called stationary signals [47]. In other words, the frequency content of stationary signals do not change in time. In this case, one does not need to know at what times frequency components exist, since all frequency components exist at all times.

When the signal is a non-stationary signal, or when the time localization of the spectral components are needed, a transform giving the Time-Frequency Representation of the signal is needed.

The *wavelet transform* is a transform of this type. It provides the time-frequency representation.[1] Often, a particular spectral component occurring at any instant can be of particular interest. In these cases it may be very beneficial to know the time intervals these particular spectral components occur. For example, the latency of an event-related potential is of particular interest (the response to a specific trigger or event), and one might be interested in the amount of time between the onset of the trigger (stimulus) and the response. So we need a transform that is capable of

[1]There are other transforms which give this information, such as short time Fourier transform, Wigner distributions, etc.

providing the time and frequency information simultaneously, hence giving the time frequency representation of the signal.

Mutiresolution Analysis and the Discrete Wavelet Transform

Like transform coding, wavelet coding is based on the premise that using a linear transform, here a wavelet transform, will result in transform coefficients that can be stored more efficiently than the pixels themselves. Due to the fact that wavelets are computationally efficient and that the wavelet basis functions are limited in duration, subdivision of the original image is unnecessary. Wavelet coding typically produces a more efficient compression than Discrete Cosine Transform (DCT) based systems, the blocking artifacts (characteristic of DCT-based systems at high compression ratios) are not present in wavelet reconstructions The choice of the wavelet to use, greatly affects the compression efficiency. For our work, we want a lightweight encoding, so we have decided to use Haar wavelets, this is described in greater detail in Section 6.2.

2.2 Background Subtraction Method for Detecting Foreground Objects

Background subtraction is a widely used approach for detecting moving objects from a static camera by differencing the current frame and a reference frame. The result highly depends on how the reference image (modeled background) represent the static scene (the scene with no moving object) of the camera view. So a good model for estimating the background is necessary for optimal result.

2.2.1 Background Model - Estimating Good Background

Several methods of performing background subtraction have been proposed in literature. These methods attempt to estimate the background model from the temporal sequence of the frames. Each of these methods have their benefits as well as

their limitations. In the following, we provide some of the common techniques that are used.

2.2.2 The Most Common Approaches of Background Generation

The approaches towards background generation range from simple ones, aiming to maximize speed and limiting the memory requirement to more sophisticated approaches aiming to achieve the highest possible accuracy.

Running Gaussian Average

Wren, *et al.* [40] has proposed to model the background independently at each (i, j) pixel location. The model is based on ideally fitting a Gaussian Probability Density Function (PDF) on the last n pixels values. In order to avoid constructing the PDF function from scratch at each new frame time, t, a running average is computed instead as:

$$\mu_t = \alpha I_t + (1 - \alpha)\mu_{t-1} \tag{2.1}$$

where I_t, is the pixels current value and μ_t the previous average; α is an empirical weight often chosen as a tradeoff between stability and quick update. The other parameter of the Gaussian PDF, the standard deviation σ_t, can be computed similarly. The advantage of the running average technique is its high computational speed and low memory requirement. For each pixel, there exists two parameters (μ_t, σ_t) instead of the buffer with the last n pixel values. The update rate of either μ_t and/or σ_t can be set to less than that of the sample (frame) rate. However, the lower the update rate of the background model, the less the system will be able to quickly respond to the actual background dynamic.

Temporal Median Filter

Several [41, 42] have proposed using a median filter to model background of the static scene from the last N frames (median value of the last N frames as the as the background model). Cucchiara, *et al.* [42] and Lo and Velastin [41] argued that a median value provides an adequate background model even if the N frames are subsampled with respect to the original frame rate by a factor of ten. In addition, Lo et. al. [42] proposed to compute the median on a special set of values containing the last N sub-sampled frames and W times the last computed median value. This combination increases the stability of the background model.

The main disadvantage of a median-based approach is that its computation requires a buffer with the recent pixel values. Moreover, the median filter does not accommodate for a rigorous statistical description and does not provide a deviation measure for adapting the subtraction threshold.

Gaussian Mixture Model

In the Running Gaussian Average background modelling technique, the background was modeled by a single distribution in each pixel. But this leads to problems when the background is not static and when there is foreground in the training data. This can be partially addressed by introducing multiple distributions. The idea is to model each surface by own distribution. This, using a number of Gaussian distribution is called *Gaussian Mixture Model*. For a greater discussion concerning the Gaussian Mixture Model see [43].

There are other models which are even more computationally intensive and memory demanding but with high accuracy. Some of them include: Kernel Density Estimation (KDE), Sequential KD approximation, Cooccurence of image variations, Eigenbackgrounds, etc [48, 49].

2.3 Security

Wireless sensor networks may operate in a hostile environment, so security is crucial to ensure the integrity and confidentiality of sensitive information [50]. To achieve this, the network need to be well protected from intrusion and spoofing. The biggest challenge in securing the network infrastructure is the constrained computation and communication capability of sensor nodes. It makes it suitable to consider nonconventional encryption techniques [52].

2.3.1 Cryptography

In cryptography, *encryption* is the process of transforming information (plaintext) using an algorithm to make it unreadable to only those possessing the secret key. The output of the transformation is called *ciphertext*. Encryption and decryption [61]. Encryption and Decryption algorithms are referred to as *cryptographic algorithms* or *cryptosystems*. Cryptanalysis refers to the breaking of a cryptosystem.

Cryptosystems can be categorized into two classes: *Symmetric key encryption* and *Asymmetric key encryption*.

Symmetric Key Encryption

Symmetric key cryptosystems (also called conventional key cryptosystems) are encryption algorithms that uses identical cryptographic keys for both encryption and decryption. Both the encryption and decryption keys are related in that they may be identical or there is a simple transformation to construct the decryption key from the encryption key.

Symmetric key algorithms can be divided in to *stream ciphers* and *block ciphers*. Stream ciphers encrypt the bytes of the message one at a time, and block ciphers take a number of bytes and encrypt them as a single unit. A Block of 64 bits was used for DES. Today the AES algorithm uses 128-bit blocks [70]. Some common ex-

amples of symmetric algorithms include Data Encryption Standard (DES), Advanced Encryption Standard (AES), RC4, TDES, etc.

Public Key Cryptosystem

The term Public Key Cryptosystems are also referred to as Asymmetric Key Cryptosystems. Unlike symmetric key algorithms, public key cryptosystem does not require a secure exchange of one or more secret key between client and server (sender and receiver). The way public key cryptography works is that one entity has the private key and keeps it safe not letting anyone else know it, the corresponding public key is made freely available. Both the keys are mathematically related in some way to each other, but at a glance, they should seem perfectly random. This makes cryptanalysis of the algorithm a much more difficult process.

Asymmetric ciphers usually are more computationally intensive than their symmetric counterparts. Common examples of asymmetric ciphers are RSA, Diffie-Hellman algorithm and Elliptic Curve Cryptosystems (ECC).

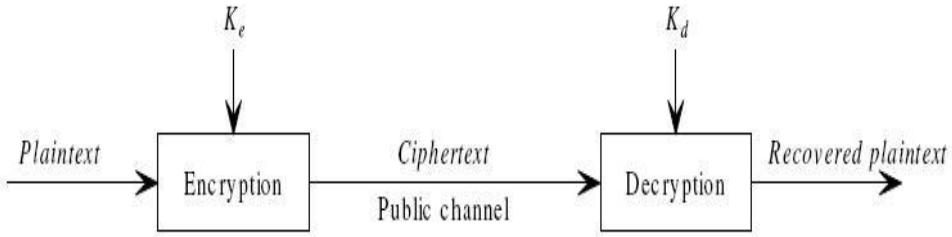

Fig. 2.1.: Encryption and decryption of a cipher

Note: For symmetric cryptosystem $k_e = k_d$, and for assymmetric (public key cryptosystem) $k_e \neq k_d$ (because it is computationally hard to compute k_d given k_e)

A cryptographically secure cipher should be secure to withstand many different attacks [53]. For most ciphers, the following four attacks are always considered:

- *Ciphertext-only attack* - attackers possess the ciphertexts only.

- *Known-plaintext attack* - attackers possess some plaintexts and the corresponding ciphertexts.
- *Chosen-plaintext attack* - attackers can select some plaintexts and get the corresponding ciphertexts.
- *Chosen-ciphertext attack* - attackers can select some ciphertexts and get the corresponding plaintexts.

It is known that many image/video encryption schemes are not secure enough against known/chosen-plaintext attacks. This will be described more in Chapter 4.

2.4 Multimedia Security

For digital rights management, confidential video conferencing, military and medical imaging system, the multimedia data has to be encrypted during storage and transmission through an open network.

2.4.1 Image/Video Encryption Scheme

The distinction between image encryption and video encryption is not prominent since most encryption techniques proposed for image are extended to encrypt videos with similar structures [54].

Some common image/video encryptions proposed in literature include:

- Almost all DCT based encryption schemes can be used to encrypt both image and video datas [55] [54].
- Entropy encoding which is used widely both in image and video encoding. the idea of making *entropy code* secret is proposed in different literatures as a security mechanism for image/video encryption. In [56, 57], the authors propose secretely permuting huffman table to encrypt the input image/video stream.

In [58] also randomly flipping the last bit of each codeword to adaptively change the Huffman table is proposed to encrypt image/video data.

- Wavelet based encryption has been suggested by many. In [59], selective bit scrambling, block shuffling, and block rotation is proposed to encrypt image/video wavelet compressed streams.

The existing or standard encryption algorithms are sometimes too intensive to be applied for encrypting multimedia data in resource starved devices like cellphone, PDA and wireless sensors. So another scheme called *Selective Encryption* is proposed [13, 72].

2.5 Selective Encryption

Selective encryption is a method of selectively concealing portions of a compressed multimedia bitstream while leaving the remaining portions of the stream unchanged [13]. This technique is widely adopted to encrypt multimedia data in resource starved devices, and aims to achieve a better tradeoff between the encryption load and the security level.

Related works and some review on selective encryption is discussed in Chapter 4. In that chapter we provide analysis concerning the insecurity of certain selective encryption schemes. Specifically we attack a selective encryption scheme that is based on shuffling spatial orientation trees of a wavelet based transform data structure.

3. SELECTIVE ENCRYPTION

3.1 Introduction

Internet multimedia applications has become extremely popular. Valuable multimedia content such as digital images and video, are vulnerable to unauthorized access while in storage as well as during a transmission over a network. Streaming of secure images/real-time video in the presence of constraints, such as bandwidth, delay, computational complexity and channel reliability is one of the most challenging problems. For example, a 512×512 color image at 24 bits/pixel would require 6.3Mbits. While the bandwidth issue can be resolved using compression, securing multimedia data still remains a big challenge, especially in light of the diversity of devices (in terms of resource availability) that will transmit and receive the content.

Traditional image and video content protection schemes are fully layered, the whole content is first compressed, and then the compressed stream is encrypted using a standard cryptographic technique (such as TDES, AES, ...) [16]. However, the requirement for high transmission rate with limited bandwidth makes this traditional technique inadequate. In the fully layered scheme compression and encryption are two different (disjoint) processes. The multimedia content is processed as a classical text assuming that all the bits in the plaintext are equally important. But with constrained resources (in real-time networking, high definition delivery, low power, low memory and computational capability) this scheme is inefficient. Thus techniques for securing multimedia data requiring less complexity and less adverse effect on the compression without compromising the security of the data is required. One such technique is to use selective encryption [4, 60]. Selective encryption is an encryption technique based on combining the encryption and compression process, that will reduce computational

complexity as well as bandwidth utilization, by encrypting only the "essential parts of the image". In Section 3.3, we briefly discuss some selective encryption techniques.

This work focuses on the analysis of a selective encryption technique that is based on the permutation (shuffling) of wavelet trees, a technique that was suggested by Kwon, et. al. [5] to be used as the sole base of providing privacy. Here we demonstrate that as the sole cryptographic primitive it is weak.

3.2 Wavelet Based Compression Techniques

Over the past several years, the wavelet transform has gained widespread acceptance in image compression research. Since there is no need to divide the image into macro blocks (no need to block the input image), wavelet based coding at higher compression avoids blocking artifacts. Wavelet transform can decompose a signal in to different subbands. There are many compression techniques that use the wavelet transform, including JPEG-2000, EZW [14] and SPIHT [12]. We now briefly discuss EZW and SPIHT.

In 1993, Shapiro [14] presented an algorithm for entropy encoding called *Embedded Zerotree Wavelet (EZW) algorithm.* After applying the wavelet transform, the coefficients can be represented using trees because of the subsampling that is performed in the transform. A coefficient in a low subband can be thought of as having four descendants in the next higher subband (see Figure 1). The four descendants each have four descendants in the next higher subband and we see a quad-tree structure emerges and every root has four leafs. A zerotree is a quad-tree of which all nodes are equal to or smaller than the root. The zero tree structure is based on the hypothesis that if a wavelet coefficient at a coarse scale is insignificant with respect to a given threshold T, then all wavelet coefficients of the same orientation in the same spatial location at finer scales are likely to be insignificant with respect to T. The idea is to define a tree of zero symbols that start at a root that is also zero and label as end-of-block. Many insignificant coefficients at higher subbands (finer resolution) can

be discarded since the tree grows as powers of four. The EZW algorithm encodes the

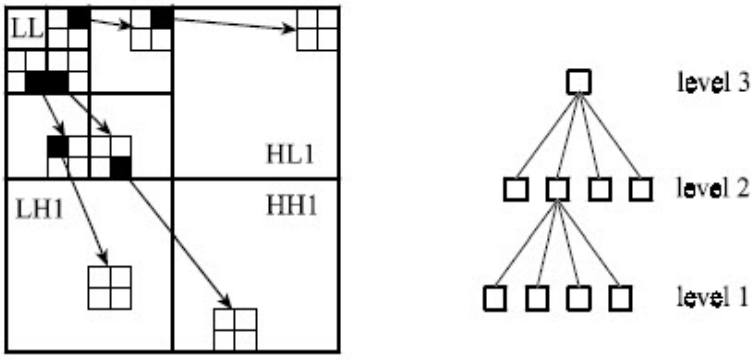

Fig. 3.1.: The relations between wavelet coefficients in different subbands as quad-trees as illustrated in [69]. LL1 is the low-low coefficients (that is, low pass filtered in the vertical, and low pass filtered in the horizontal). LH1,HL1,HH1 are defined similarly.

obtained tree structure. The resulting output is such that the bits that are generated in order of importance, yielding a fully embedded code. The main advantage of this encoding technique is the encoder can terminate the encoding at any point, thereby allowing one to achieve a target bit rate (i.e. rate scalable). Similarly, the decoder can also stop decoding at any point resulting an image that would have been produced at the rate of the truncated bit stream. Since EZW generate bits in order of importance, those bits that affect the perceived quality of the decompressed image/video most can be placed at the beginning of the data stream; since the entire stream depends on those bits they can be a good candidate for selective encryption.

In 1996, Said and Pearlman [12] introduced a computationally simple compression technique (algorithm) called *SPIHT (Set Partitioning In Hierarchical Trees)* that is based on the wavelet transform. SPIHT uses set partitioning and significance testing on hierarchical structures of transformed images to extend/improve on the work of

Shapiro [14]. SPIHT is also a good candidate to be used in a selective encryption scheme.

3.3 Prior Work on Selective Encryption

Selective encryption has been suggested and adopted as a basic idea for encryption of digital images and videos, aiming to achieve a better trade off between the encryption load and the security level. Selective encryption is a method of selectively concealing portions of a compressed multimedia bitstream while leaving the remaining portions of the stream unchanged.

There are a number of selective encryption techniques. Here we briefly discuss only a few schemes. For more details and a more thorough discussion we suggest the reader look at [7, 60].

In 2002, Podesser, Schmidt and Uhl [10] applied the following technique. They proposed a selective bitplane encryption using AES. They conducted a series of experiments on 8-bit grayscale images, and observed the following: (1) encrypting only the MSB is not secure; a replacement attack is possible, (2) encrypting the first two MSBs gives hard visual degradation, and (3) encrypting three bitplanes gives very hard visual degradation.

Zeng and Lei [71] proposed a selective encryption scheme in the frequency domain (wavelet domain). The general scheme consists of selective scrambling of coefficients by using different primitives (selective bit scrambling, block shuffling, and/or rotation). The input video frames are transformed using wavelet transform and each subband represents selected spatial frequency information of the input video frame. The authors propose two ways to scramble the coefficients. In their first suggestion, they observed that some bits of the transform coefficients have high entropy and can thus be encrypted without greatly affecting compressibility. In their second suggestion, the authors observed that shuffling the arrangement of coefficients in a transform coefficient map can provide effective security without destroying compressibility, as

long as the shuffling does not destroy the low-entropy aspects of the map relied upon by the bitstream coder. To increase security, the authors suggested block shuffling. Each subband is divided into a number of blocks of equal size (the size of the block can vary for different subbands) and within each subband, blocks of coefficients will be shuffled according to a shuffling table generated using a key.

Kwon, Lee, Kim, Jin, and Ko [5] described a scheme which involves shuffling of spatial orientation trees (SOT) to secure multimedia data. The authors mentioned the deficiency of traditional block shuffling technique and proposed *wavelet tree shuffling* as an alternate security mechanism as part of the security architecture for multimedia digital rights management. The authors proposed a 4-level wavelet transform. According to Shapiro's [14] algorithm, this will result in 13 sub-bands, and the wavelet coefficients are grouped according to wavelet trees.

In 2005, Salama and King [13] proposed a joint encryption-compression technique (Selective Encryption) for securing multimedia data based on the EZW compression scheme. Their approach is selectively encrypting those bits for which the entire bit stream depends. Through a serious of experiments/simulations, the authors found that encrypting the leading 256 bits of a 512×512 image will provide sufficient security. In their scheme, first the image will be transformed using discrete wavelet transform, apply EZW, and then entropy encoded before it is encrypted using the proposed Selective Encryption technique. The authors developed a security analysis of the proposed joint compression-encryption technique, and demonstrated an attack called *Database Attack*. In this attack, an adversary (unintended receiver) can intercept the encrypted signal and attempt to replace the encrypted portion of the data stream by another portion that he/she would generate. For the attack to be successful, the interceptor would need a selective database (small enough for computations to be feasible and large enough to include all possible target images), that contains at least one of the possible images that can be transmitted. The attacker then performs a brute force attack by encoding all images in the database and comparing the unprotected part of the stream with the corresponding part of the compressed images

from the database. If there is a match, the attacker can replace one stream with another. As a countermeasure to this attack, the authors propose *Randomly shuffling the SOT prior to encoding*, shuffling the SOT (spatial orientation trees) after wavelet transform. This will frustrate brute force database attack without affecting the compression performance.

In 2006, Wu and Mao [8] proposed a shuffling technique as part of their selective encryption architecture. The authors use the MPEG-4 fine granularity scalability (FGS) functionality provided by the MPEG-4 streaming video profile [6] to illustrate their concept and approach. A video is first encoded into two layers, a base layer that provides a basic quality level at a low bit rate and an enhancement layer that provides successive refinement. The enhancement layer is encoded bitplane by bitplane from the most significant bitplane to the least significant one to achieve fine granularity scalability. The authors propose an intra bit plan shuffling on each bit plane of n-bits according to a set of cryptographically secure shuffle tables and using a run-EOP approach. In addition to bit-plane shuffling, the authors also proposed randomly flipping the sign bit s_i of each coefficient according to a pseudo-random bit b_i from a one-time pad, i.e., the sign remains the same when $b_i = 0$ and changes when $b_i = 1$.

4. ATTACKING WAVELET TREE SHUFFLING ENCRYPTION SCHEME

In this chapter, we are analyzing shuffling of the wavelet trees (SOT's) as if it were the only mechanism used for encryption. First we describe what a generic wavelet tree shuffling encryption scheme would be, as discussed in [5].

4.1 A Generic Framework of a Wavelet Tree Shuffling Encryption Scheme

Here we outline the construction of an encryption scheme which is based on the use of permuting the trees which are produced by the wavelet transform. This scheme was suggested by Kwon et. al. in [5].

Suppose the image I is of size $M \times N$. Then I can be represented as

$$I = \begin{bmatrix} m_{0,0} & \cdots & m_{0,N-1} \\ \vdots & \ddots & \vdots \\ m_{M-1,0} & \cdots & m_{M-1,N-1} \end{bmatrix}_{M \times N} \tag{4.1}$$

where $m_{i,j}$ is the i, j pixel of I.

For a level L of wavelet decomposition the number of SOT's (spatial orientation tree) is

$$T = \frac{M \cdot N}{2^{2L}} \tag{4.2}$$

If $M = 2^d$ then the maximum level of decomposition will be d. Thus, if an image I of size 512×512 is decomposed using 4 levels of decomposition then there will be 1024 trees. Since there are 1024! permutations of the trees, this would require a key of at least 1024 bits. A symmetric cryptosystem which uses a key of size 1024 should provide security for well over 50 years [1, 2]. However such a scheme does not possess such security.

Encryption:

In this procedure, the coefficient matrix I of size $M \times N$ is shuffled using a permutation (determined by symmetric key K) to form a corresponding image C. This is achieved by applying a permutation (shuffling) to the SOT's that were created during the wavelet transform. More formally let $\mathcal{WT}$ denote the 2D discrete wavelet transform and PERM_K denote the permutation that shuffles the wavelet trees. Then the ciphertext C is generated as follows:

First the wavelet transform is applied to I,

$$\mathcal{WT}(I) = (\mathcal{T}_1, \mathcal{T}_2, \ldots, \mathcal{T}_T)$$

(here $\mathcal{T}_i$ denotes the i^{th} tree produced by the wavelet transform). Then given key K, the trees $(\mathcal{T}_1, \mathcal{T}_2, \ldots, \mathcal{T}_T)$ are then permuted as

$$C = \text{PERM}_K(\mathcal{T}_1, \mathcal{T}_2, \ldots, \mathcal{T}_T).$$

This process is illustrated in Fig. 4.1.

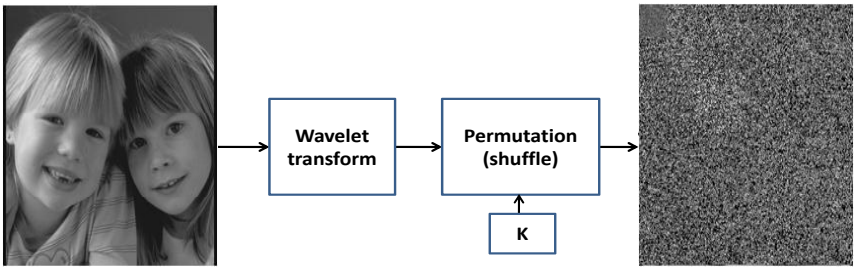

Fig. 4.1.: Encrypting by shuffling wavelet trees

Decryption:

Given the ciphertext C, the image I is then reconstructed as follows. First the inverse of the permutation (that was induced by key K) is applied. Thus

$$(\mathcal{T}_1, \mathcal{T}_2, \ldots, \mathcal{T}_T) = \text{PERM}_K^{-1}(C).$$

Then the $\mathcal{IWT}$ (inverse wavelet transform) is applied. The result is

$$I = \mathcal{IWT}(\mathcal{T}_1, \mathcal{T}_2, \ldots, \mathcal{T}_T).$$

4.2 Attacking a Wavelet Tree Shuffling Encryption Scheme

In this work, we are analyzing shuffling of the wavelet trees (SOT's) as if it were the only mechanism used for encryption [5].

Norcern and Uhl [9] also discussed the insecurity of a system (in terms of compression performance) that was based on randomly permuting wavelet-subbands incorporated in the JPEG2000 or the SPIHT coder proposed by Uehara et. al. in [17]. Their work differs from ours in the sense that they were attacking a scheme that was randomly permuting the coefficients of wavelet subbands, while our attack is on encryption schemes that are shuffling the tree structure created after the wavelet transform.

The basis of our attack will be a chosen plaintext attack, in particular a lunch time attack We will assume that the attacker has temporary possession of the encryption machine and can feed the machine selected plaintext and will receive the corresponding ciphertext. From this lunch time attack the adversary will be able to determine the permutation (encryption) key.

First consider an image of size $\mathbf{M} \times \mathbf{N}$ and suppose it is transformed in to wavelet coefficients using the L-level discrete wavelet transform (DWT). With an L-level decomposition, we have $3L + 1$ frequency bands. In Fig 4.4, when $L = 4$, the lowest frequency subband is located in the top left (i.e., the LL4 subband, and the highest frequency subband is at the bottom right (i.e., the HH1 subband). The relation

between this frequency bands can be seen as a parent-child relationship [14]. Thus, for an image of size $M \times N$ with L-level of decomposition, in total we will have $\frac{M}{2^L} \cdot \frac{N}{2^L}$ trees. After constructing wavelet trees, a secret key K is used to randomly shuffle the trees.

Clearly if an attacker can guess the size of the image and the number of levels of decomposition, then shuffling of the wavelet trees (SOT's) is vulnerable to the lunch time attack. A simple scenario of a lunch time attack: a legitimate user s away from the desk (computer) without locking their computer/machine, the attackers can use a chosen plaintext attack. A chosen plaintext attack can be launched by any party (adversary) who can access the machine while the user is absent. For the attack to be successful, the adversary needs to have access for the encryption machine. Once the adversary has access to the encryption machine, he/she can choose a series of chosen plaintexts and feed them to the encryption machine as shown in Fig. 4.5. Thus if I_j denotes a chosen plaintext, and if we denote the wavelet tree shuffling encryption scheme (as illustrated in Fig 4.1) by $E(I_j, K)$ where K is the key, then the adversary will generate chosen plaintexts

$$E(I_1, K), E(I_2, K), \ldots, E(I_r, K).$$

The adversary can use these to determine the image size and the level of decomposition. Thus we will assume that the adversary knows these parameters.

In [5], Kwon et. al. proposed the shuffling of wavelet trees of a wavelet coefficient which undergoes 4-levels of wavelet decomposition as part of their security architecture for digital rights management. For an image of size 512×512 which undergoes 4-levels of wavelet decomposition, there will be 1024 trees according to Equation 4.2 . And shuffling of these trees using a randomized shuffling key (shuffling matrix) should provide a security of 1024 bit key size.

Though Kwon et. al. [5] were using a level $L = 4$ of decomposition for an image of size 512×512, we will provide an analysis/experiments based on image size of 256×256. Only a slight modification of our experiments would have to be constructed

to attack an image of size 512×512. The following table demonstrates the relationship between the level of decomposition and the number of trees.

Table 4.1: Relationship between no. of decomp. and no. of trees for an image of size 256×256

No. of decomp.	No. of trees
3	1024
4	256
5	64
6	8
7	4

Assume for the moment that the level of decomposition was $L = 5$. In Fig 4.2, we provide the original chosen plaintext image. This image was selected, an image consisting of a series of integers from 1 to 64, where each integer is in white placed within a small back box, in order to clearly determine the permutation key and the levels of decomposition. Using the encryption machine, and applying the shuffle to this plaintext we get the ciphertext in Fig 4.3, for a level of decomposition $L = 3$, we get the ciphertext in Fig 4.4, for a level of decomposition $L = 4$, and we get the ciphertext in Fig 4.5, for a level of decomposition $L = 5$. Observe the clarity of the image Fig 4.5, the digits are clearly visible thus revealing that we have determined the level of decomposition. Once the adversary possesses Fig 4.5, they know the level of decomposition as we well as the permutation, hence they know the key, and so they have broken the cipher.

So due to the nature of wavelet trees if an adversary would have guessed the correct size of the image and the number of level of decomposition, he/she can get a ciphertext that will leak information about the randomized key used to shuffle the wavelet trees (SOT's). The adversary needs to encrypt only $\log_2(V)$ times for

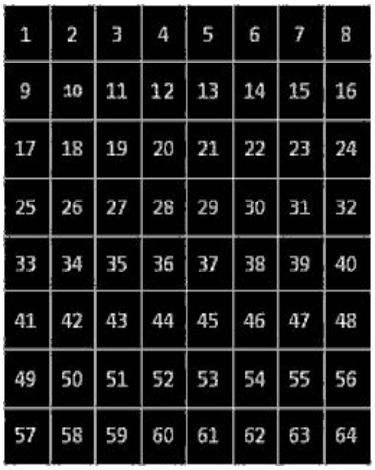

Fig. 4.2.: Original image

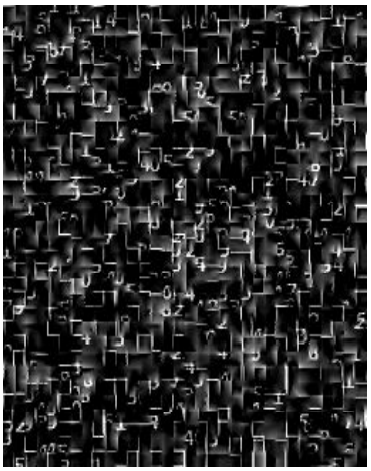

Fig. 4.3.: Shuffled image where $L = 3$

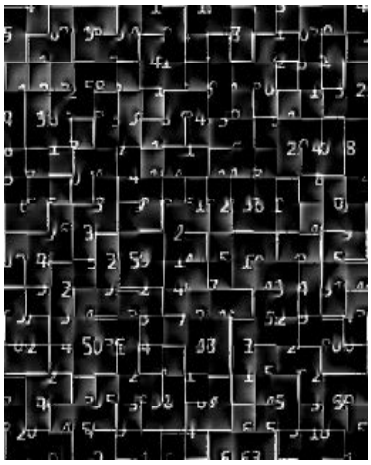

Fig. 4.4.: Shuffled image where $L = 4$

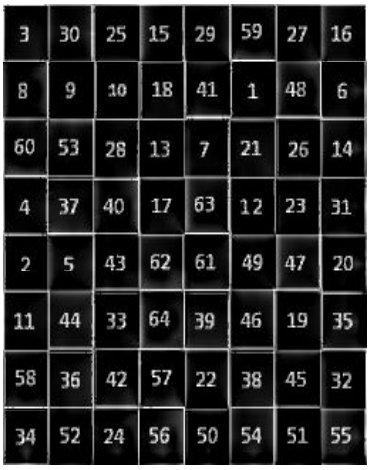

Fig. 4.5.: Shuffled image where $L = 5$

each carefully chosen plaintext images to find the key, where V is $max(M, N)$ for an image of size $M \times N$. This is because the maximum number of possible levels of decomposition is bounded by the logarithm of the dimensions as observed in Section 4.1. An image of size 256×256 has at most 8 levels of decomposition, as illustrated in the above figures, by the choosing an appropriate plaintext, and viewing the potential ciphertexts from the vantage of different levels of wavelet decomposition (such as $L = 3$, $L = 4$, $L = 5$), the correct level and key can be determined. That is, the image is a carefully chosen image, determined by the adversary and the resulting

ciphertext (Fig. 4.3, 4.4, 4.5) will be analyzed, and if the adversary can easily deduce how the wavelet trees are shuffled then they have found the key. For example, for an image of size 256×256 which has gone through 4 levels of wavelet decomposition we need to run the encryption machine for the chosen plaintext at most 8 times and as it can be easily be seen how the trees are shuffled by looking at Fig 4.5. The series of chosen plaintext (image) used by the adversary will be limited since the possible number of decomposition are limited (small numbers) to distort the image visually. For example, for an image of size 512×512 a wavelet transform of the image with 8 level of decomposition will have only 4 wavelet trees and the key size to shuffle these trees also be 4, and will not distort the image. Thus, the adversary can easily guess the key used to shuffle the wavelet trees.

We have discussed the wavelet tree shuffling encryption scheme [5]. We have showed that the shuffling of the wavelet trees, when used as a sole security mechanism, is insecure against a chosen plaintext attack. However despite its weaknesses, shuffling of wavelet trees can add security when other cryptographic primitives are used. For example, in [13] the authors use wavelet tree shuffling as a supplementary security mechanism to strengthen the security of multimedia data (to protect against the *database attack*).

5. DESIGN MODEL

5.1 Introduction - Design Summary

Signal processing applications in wireless sensor networks need to consider resource constraints. With high energy cost for wireless communications, application algorithms should be designed to reduce communication cost. Sensor readings are highly correlated spatially and temporally. Effective exploitation of these correlations can reduce data communication cost significantly. In most sensor applications, events are not occurring in a consecutive manner. Therefore, it is a waste of energy to keep nodes active for periods when no events are happening.

In our work, we investigated energy efficiency and power awareness in wireless sensor networks. Although for efficient energy operation of sensors, both the networking protocol and signal processing algorithms have to be optimized. Our work concerns devising signal processing algorithms and modifying some of the existing signal processing algorithms to fit the application (to be feasible to be used under resource constraint), as well as support energy efficient operations in wireless sensor networks. We constructed an overall design of how the encoder and decoder will interact. Lastly, we have verified the effectiveness and energy efficiency of our algorithms via simulations.

5.2 Design Goal

Compression of Sensor Readings

In our work we will use

1. *Integer based Haar wavelet transform* and *run-length based coding* of sensor readings without taking into account spatial correlation.

2. We have also considered Background Subtraction. This is proposed for lightweight encoding of sensor readings, for situations where images are correlated temporally.

3. We construct an encoder/decoder design that switches compression mode between using Discrete Wavelet Transform (DWT) and using Background Subtraction based on feedback/directions from the decoder.

Exploiting Correlation of Sensor Readings

We intend to construct an encoding scheme that reverses the traditional balance of complex encoder and simple decoder is proposed. It uses Block Matching Algorithm (BMA) to quantify spatial correlation of readings of proximate sensors at the decoder side and send the parameters using backward channel optimize the encoder. It has recently been shown [34] that the traditional balance of complex encoder and simple decoder can be reversed within the framework of the so-called distributed source coding, which exploits the source statistics at the decoder, and by shifting the complexity at this end, allows the use of simple encoders. Clearly, such algorithms are very promising for WMSNs and specially for networks of video sensors, where it may not be feasible to use existing video encoders at the source node due to processing and energy constraints. Inspired by this idea and a work by Delp et. al. [29], we have designed a system that will shift some of the computationally intensive operations of the encoder to the decoder side and use the backward channel to send parameters to the encoder.

Because we will use a number of compression techniques our sensors need to get feedback from the decoder concerning the quality of images. Consequently we introduce a Reduced-Reference quality assessment method is proposed to measure quality of the reconstructed image with out having the original image. It uses some statistics about the original image as a side information to assess the quality of the reconstructed image.

Remark: Although every operation at all level of the network has to be optimized for energy efficiency (such as Power Aware Computing, Power Management by Radios, Energy Aware Packet Forwarding, Energy Aware Wireless Communication, Traffic Distribution, Topology Management etc), in our work here we focus on power saving due to efficient signal processing.

5.3 Where Does the Power Go?

The system architecture of a wireless sensor node is comprised of four subsystems: (i) a computing subsystem consisting of a microprocessor or microcontroller, (ii) a communication subsystem consisting of a short range radio for wireless communication, (iii) a sensing subsystem that links the node to the physical world and consists of a group of sensors and actuators, and (iv) a power supply subsystem, which houses the battery and the DC-DC converter, and powers the rest of the node [36]. Each subsystem of the sensor, consumes energy at a different level, so an efficient algorithm has to be designed to control the energy dissipation in each subunit.

Radio communication dissipates significantly more energy compared to computation in sensor nodes [26, 28, 30]. As sensor networks are severely constrained by energy (sensor nodes are battery-driven, and hence operate on an extremely tight energy budget), it is important to reduce communication energy. Compressing data to reduce the number of bits to be sent is a good approach to reduce communication energy dissipation in sensor networks. One common application of wireless sensor networks is event tracking, which has widespread use in applications such as security and battle field surveillance, medical and health services, wildlife habitat monitoring, as well as several others. Tracking involves a significant amount of collaboration between individual sensors to perform complex signal processing algorithms such as Filtering, Data Fusion, and Coherent Beam forming. This collaborative signal processing nature of sensor networks offers significant opportunities for energy management. For example, just the decision of whether to use the collaborative signal processing at

the user end-point or somewhere inside the network has significant implication on energy and lifetime, and our work, as described in Section 8.1.2, concerns exploiting spatial correlation between neighborhood sensors at the base station side. We use tracking/surveillance as our target application to motivate many of the techniques presented in our research here. In general, sensor readings from near-by sensors are correlated in space. Rather than straight data compression, spatial correlation can be exploited to achieve improved data compression. The distributed source coding problem of correlated sources has been studied extensively [53, 44, 25, 22].

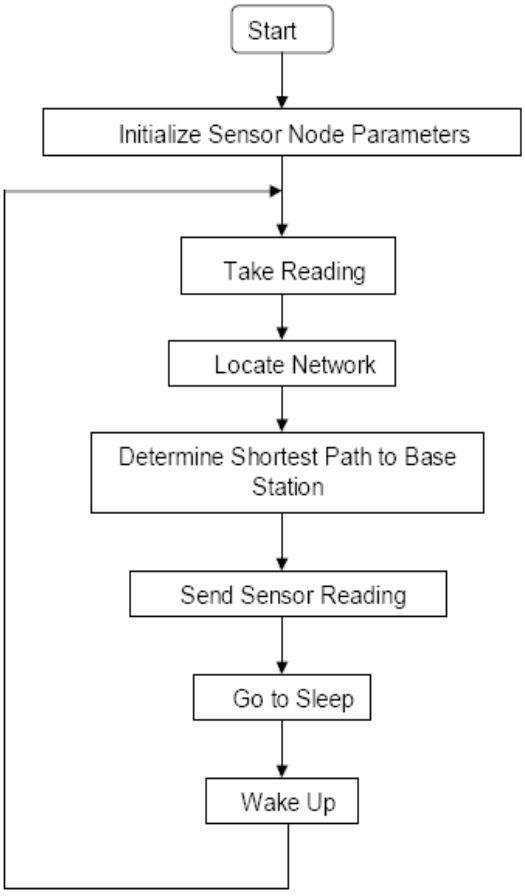

Fig. 5.1.: Sensor operation flowchart

5.4 Energy/Power Analysis of Sensor Nodes

5.4.1 In-Sensor (Node Level) Energy Optimization

Integer Based Haar Wavelet Transform: The Haar transform is the simplest of the wavelet transforms. This transform cross-multiplies a function against the Haar wavelet with various shifts and stretches. The Haar basis vectors are constructed by a process of dilation (squeezing) and shifting. These vectors are perpendicular to each other; even though these basis vectors are orthogonal, they are not orthonormal. However, we can easily normalize them by calculating the magnitude of each of these vectors and then dividing their components by that magnitude. But for light weight computation of the Haar transform we used the following the following equations:

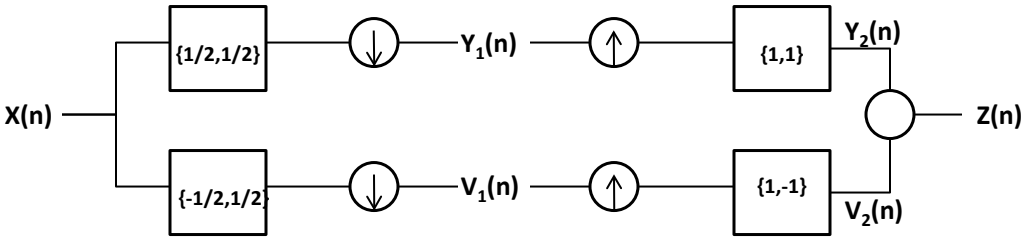

Fig. 5.2.: Averaging and differencing to find Haar vectors

Analysis and synthesis filter bank for 1 level of wavelet decomposition using integer based Haar wavelets.

$$
\begin{aligned}
Y_1(n) &= \frac{X(2n) + X(2n+1)}{2} \\
V_1(n) &= \frac{X(2n) - X(2n+1)}{2} \\
Y_2(n) &= Y_1(n) + Y_1(n-1) \\
V_2(n) &= V_1(n) - V_1(n-1) \\
Y_2(n) &= \frac{1}{2}[X(2n) + X(2n+1)] + \frac{1}{2}[X(2n-2) + X(2n-1)] \\
V_2(n) &= \frac{1}{2}[X(2n) - X(2n+1)] - \frac{1}{2}[X(2n-2) - X(2n-1)]
\end{aligned}
$$

where $X(n)$ is the original signal, $Y_1(n)$ and $V_1(n)$ are the decimated version of the low-pass and high-pass coefficients respectively (analysis filter); and $Y_2(n)$ and $V_2(n)$ are the interpolated version of the low-pass and high-pass coefficients respectively (synthesis filter).

5.4.2 Network-Wide Energy Optimization

Traffic Distribution: One aspect of traffic forwarding is the choice of an energy efficient multi-hop route between source and destination. Several approaches have been proposed [37, 38] which aim at selecting a path that minimizes the total energy consumption. However, such a strategy does not always maximize the network lifetime [39]. So although the shortest path towards the base station seems the best way, it has to be carefully studied to distribute the traffic for more optimal packet forwarding.

5.5 System Model

We model the network as a tree graph $G(\mathcal{N}, L)$, where $\mathcal{N}$ represents the set of entities in the network, $|\mathcal{N}|-1$ sensor nodes and a single sink (also called *base station*). L is the set of direct wireless communication links present between any node pairs. Processing for compression is performed for the locally sensed data at each of the sensor nodes, and sent to the base station in a multi-hop scheme. An example sensor network with 7 sensors and a base station is given in Fig. 5.4

5.6 Network Assumption

In defining our model, the following assumptions are made: Computation and communication are assumed to occur simultaneously as supported by various platforms (e.g. $CC24301$ from Texas Instruments and $MC13213$ from Freescale. [35] Freescale). Computation delay is assumed to be negligible compared to the commu-

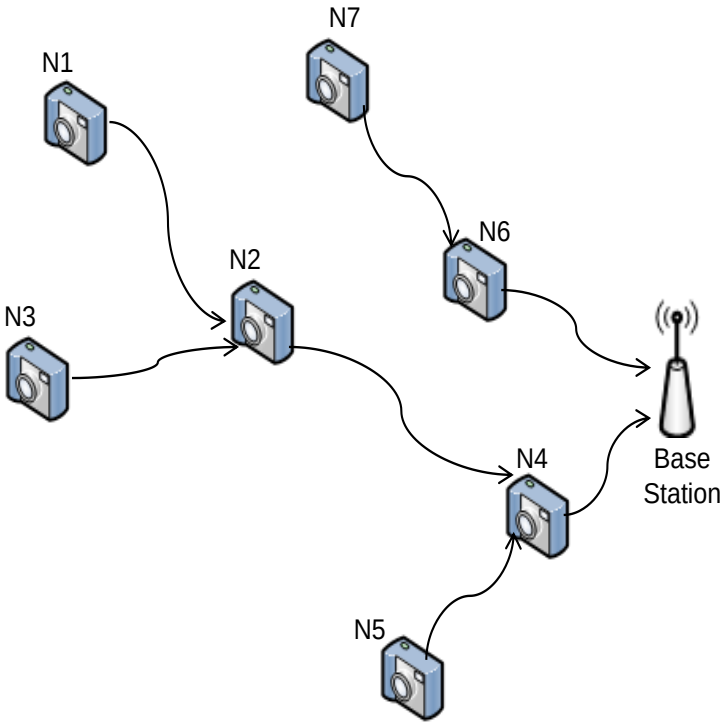

Fig. 5.3.: WMSN with 7 sensors and a single sink

nication delay, which is true for many architectures in practical use today. At startup each of the nodes has the same amount of energy available.

5.7 Node Power Consumption Model

Energy cost is instantaneous power consumption accumulated over time. The objective of network lifetime maximization can be achieved indirectly by minimizing the nodal power dissipation. An essential goal of our work, is to achieve the objective of the network lifetime maximization.

To estimate of the total power consumption, we have to consider the communication and computation power consumption components at each of the sensor nodes As described in [26], the radio module energy dissipation can be characterized into two types. The first is given by $E_{elec}(J/b)$, the energy dissipated to run the transmit

or receive electronics and the second is given by $\varepsilon_{amp}(J/b/m2)$, the energy dissipated by the transmit power amplifier to achieve an acceptable E_b/N_o at the receiver. We assume d^2 energy loss for transmission between sensors (assuming the distances between sensors are relatively short) [27]. To transmit a k-bit packet a distance, d, the energy dissipated is:

$$E_{tx}(k,d) = E_{elec} \cdot k + \varepsilon_{amp} \cdot k \cdot d^2 \tag{5.1}$$

and to receive the $k - bit$ packet, the radio expends

$$E_{rx}(k) = E_{elec} \cdot k \tag{5.2}$$

For μAmp wireless sensor, $E_{elec} = 50nJ/b$ and $\varepsilon_{amp} = 100pJ/b/m2$ [26]. To prolong the lifetime of the wireless sensor all aspects of the sensor system should be energy efficient. There should be efficient network protocol layer and efficient signal processing algorithm. Our work fconcerns the energy dissipated at the radio and communication module, in particular, local energy efficient signal processing.

5.8 Our First Design

Our first design of the encoding system describes the general encoding procedure using the figure given below. The system operates in two different encoding modes, one at a time by switching mode according to the feedback metrics given by the decision box or the Base Station to optimize the encoding system. The detail mode of operation for the encoding system along with more optimization is given in Section 6.4.3.

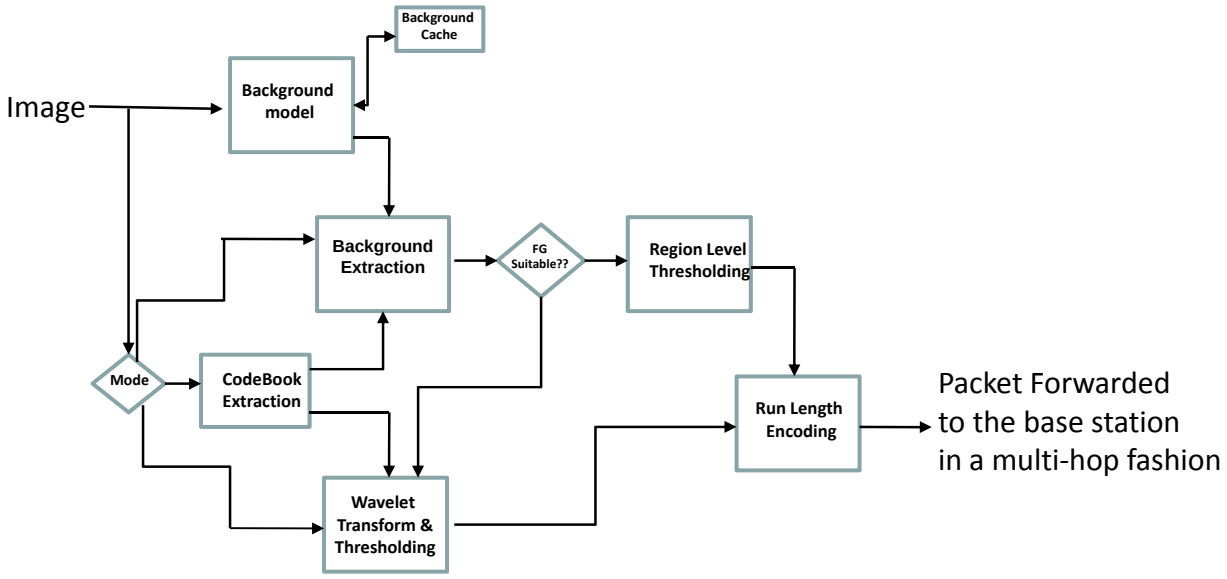

Fig. 5.4.: A fist design of our encoder

6. ENCODER

6.1 Introduction

For both archiving, as well as transmission through the network multimedia data has to be compressed. The principal approach in image compression is the reduction of the amount of image data(bits) while preserving information (image details).

6.1.1 Principles of Image Compression

A common characteristic of images is that the neighboring pixels are correlated and thus hold redundant information. A mathematical operation can be performed to determine the uncorrelated representations within the image. Two elementary components of compression are redundancy reduction and irrelevancy reduction. Redundancy reduction aims at removing duplication from the signal source image. Irrelevancy reduction omits parts of the signal that is not noticed by the signal receiver, namely the Human Visual System (HVS). In general, three types of redundancy can be identified: (a) Spatial Redundancy or correlation between neighboring pixel values, (b) Spectral Redundancy or correlation between different color planes or spectral bands and (c) Temporal Redundancy or correlation between adjacent frames in a sequence of images specially in video applications. Image compression research aims at reducing the number of bits needed to represent an image by removing the spatial and spectral redundancies as much as possible.

6.1.2 Classification of Compression Technique

There are two ways that we can consider for classifying compression techniques-lossless vs. lossy compression and predictive vs. transform coding.

Lossless vs. Lossy Compression

In lossless compression schemes, the reconstructed image, after compression, is numerically identical to the original image. However lossless compression can only achieve a modest amount of compression. An image reconstructed following lossy compression contains degradation relative to the original. Often this is because the compression scheme completely discards redundant information. However, lossy schemes are capable of achieving much higher compression. Under normal viewing conditions, no visible loss is perceived (visually lossless). In our target application, we will be processing surveillance images, so the compression type will definitely be lossy.

In our target application, we will be transmitting surveillance images. Thus a lossy compression is very appropriate.

Predictive vs. Transform Coding

In *predictive coding*, information already sent or available is used to predict future values, and the difference is coded. Since this is done in the image or spatial domain, it is relatively simple to implement and is readily adapted to local image characteristics. Differential Pulse Code Modulation (DPCM) is one particular example of predictive coding. *Transform coding*, on the other hand, first transforms the image from its spatial domain representation to a different type of representation using some well-known transform and then codes the transformed values (coefficients). This method provides greater data compression compared to predictive methods, although at the expense of greater computation [20].

6.1.3 Model/Framework of General Image Compression Method

A typical lossy image compression system is shown in Fig.6.1. It consists of three closely connected components namely (a) Source Encoder, (b) Quantizer and (c)

Entropy Encoder [20]. Compression is achieved by applying a linear transform in order to decorrelate the image data, quantizing the resulting transform coefficients and entropy coding the quantized values.

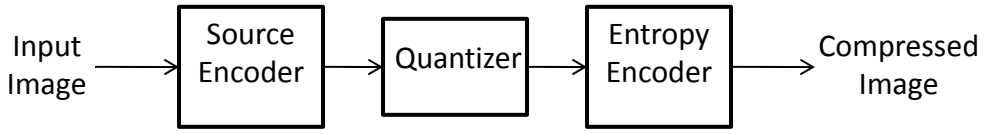

Fig. 6.1.: A model for lossy image encoder

Source Encoder (Linear Transformer)

A variety of linear transforms have been developed which include Discrete Fourier Transform (DFT), Discrete Cosine Transform (DCT), Discrete Wavelet Transform (DWT) and many more, each with its own advantages and disadvantages.

Quantizer

A quantizer is used to reduce the number of bits needed to store the transformed coefficients by reducing the precision of those values. As it is a many-to-one mapping, it is a lossy process and is the main source of compression in an encoder. Quantization can be performed on each individual coefficient, which is called Scalar Quantization (SQ). Quantization can also be applied on a group of coefficients together known as Vector Quantization (VQ) [21]. Both uniform and non-uniform quantizers can be used depending on the problems.

Entropy Encoder

An entropy encoder supplementary compresses the quantized values losslessly to provide a better overall compression. It uses a model to perfectly determine the

probabilities for each quantized value and produces an appropriate code based on these probabilities so that the resultant output code stream is smaller than the input stream. The most commonly used entropy encoders are the Huffman encoders and the Arithmetic encoder. For applications requiring fast execution, Run Length Encoding (RLE) is very effective [22]. For our research we used Run Length Encoding, for it is lightweight encoding.

A properly designed quantizer and entropy encoder are absolutely necessary along with optimum signal transformation to get the best possible compression. As noted above, our choice of an entropy encoder was Run Length Encoding (RLE) for its speed and energy efficient implementation (computations), since it will be implemented in a resource constrained device (wireless multimedia sensors).

6.1.4 Wavelets for Image Compression

The wavelet transform exploits both the spatial and frequency correlation of data by dilations (or contractions) and translations of mother wavelet on the input data. It supports the multi-resolution analysis of data i.e. it can be applied to different scales according to the details required, which allows progressive transmission and zooming of the image without the need of extra storage. Another encouraging feature of wavelet transform is its symmetric nature that is both the forward and the inverse transform has the same complexity, building fast compression and decompression routines. Its characteristics well suited for image compression include the ability to take into account of Human Visual Systems (HVS) characteristics, very good energy compaction capabilities, robustness under transmission, high compression ratio etc. The implementation of wavelet compression scheme is very similar to that of subband coding scheme: the signal is decomposed using filter banks. The output of the filter banks is down-sampled, quantized, and encoded. The decoder decodes the coded representation, up-samples and recomposes the signal.

Wavelet transform divides the information of an image into approximation and detail subsignals. The approximation subsignal shows the general trend of pixel values and other three detail subsignals show the vertical, horizontal and diagonal details or changes in the images. If these details are very small, then they can be set to zero (i.e. below some threshold) without significantly changing the image. The greater the number of zeros the greater the compression ratio. If the energy retained (amount of information retained by an image after compression and decompression) is 100% then the compression is lossless as the image can be reconstructed exactly. This occurs when the threshold value is set to zero, meaning that the details have not been changed. If any value is changed then energy will be lost and thus lossy compression occurs. As more zeros are obtained, more energy is lost. Therefore, a balance between the two needs to be found out.

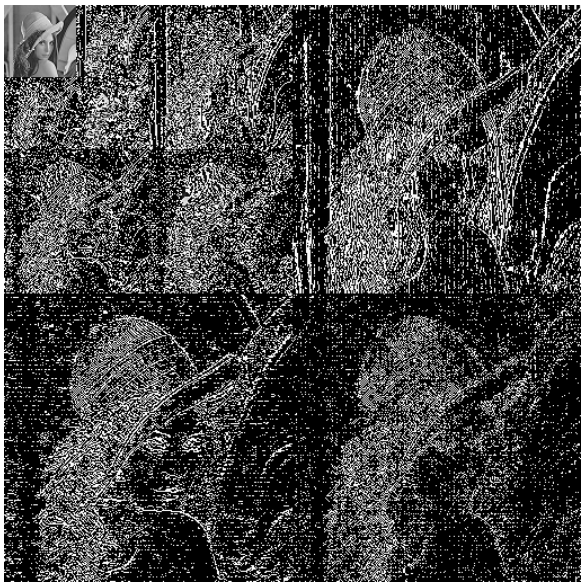

Fig. 6.2.: Wavelet decomposition of Lena (512×512, $L = 3$)

6.2 Haar Wavelet Technique

The Haar transform decomposes a discrete signal into two subsignals, each half of its original length. One subsignal is a running average or *trend*; the other signal is a running difference or *fluctuation* [46].

For a discrete signal of the form,

$$f = (f_1, f_2, ..., f_N)$$

where N is a positive even integer which we shall refer to as the length of f. The values of f are the N real numbers $f_1, f_2, ..., f_N$.

The first *trend*, $\mathbf{a}^1 = (a_1, a_2, ..., a_{N/2})$, for the signal f is computed by taking a running average in the following way. Its first value, a_1 is computed by taking the average of the first pair of values of f, i.e.: $a_1 = (f_1 + f_2)/2$. Similarly, a_2 is computed as $a_2 = (f_3 + f_4)/2$. Subsequent terms are computed in a similar fashion, i.e.

$$a_m = \frac{f_{2m-1} + f_{2m}}{2}$$

for $m = 1, 2, 3, ..., N/2$.

The other subsignal called fluctuation (detail coefficient) is denoted by $\mathbf{d}^1 = (d_1, d_2, ..., d_{N/2})$. It is computed as a running difference in the following way. Its first value d_1 is found by taking half the difference of the first pairs of values of f, that is, $d_1 = (f_1 - f_2)/2$. Continuing in this manner,

$$d_m = \frac{f_{2m-1} - f_{2m}}{2} \tag{6.1}$$

for $m = 1, 2, 3, ..., N/2$.

6.2.1 Haar Example

Given four points of data, say values of a pixel in an image, the Haar wavelet can be used to compress this data through a process called averaging and differencing.
Pixel values: {9, 7, 3, 5}

$(9 + 7)/2 = 8$, $(9 - 7)/2 = 1$

$(3+5)/2 = 4$, $(3-5)/2 = -1$

Coefficients: {8, 4, 1, ,1}

$(8+4)/2 = 6$, $(8-4)/2 = 2$

Coefficients: {6 , 2, 1, 1}

There are two types of data here, sparse data and detailed data. The sparse data is what we want to remove (in this example are the numbers {9,7,3,5,8,4,6}). The other data are the details which make up the differences when doing our compression (in this example they are {2,1,-1}).

But what good is compression that takes four values and compresses it to four values? Simple, pixel values of images are similar to their neighbors. If not we would be looking at random pixels and there would not be an object. When doing the averaging and differencing with wavelets, the detail values are usually low numbers and sometimes zero. These detail values (which compose all but one of the resulting values) can be compressed much better than the original pixel values. In this example, the number {6 2 1 1} are more easily compressible than {9 7 3 5}.

6.2.2 Filter Banks

As discussed above, there are two kinds of data, the sparse data and the detailed data. Coefficients are extracted from the original set of number by using two kinds of filters, high pass (details) and low pass (average). After the two filters are applied, the filtered data from the high pass filter is stored as coefficients for later reconstruction of the signal. The filtered data from the low pass filter is now treated as the original data and the low and high pass filters are then applied to this data. This is repeated until the filtered data from the low pass filter outputs only one number.

6.2.3 Image Thresholding

The main concept of the wavelet transform is: that regions of little variation in the original image reveal themselves as small or zero elements in the wavelet trans-

formed version. The zeros are due to the occurrences of identical adjacent elements in the original matrix. The coefficient matrix we get after the wavelet transform will definitely be a sparse matrix (i.e.: with a high proportion of zero entries). For most image matrices, their corresponding wavelet transformed versions are much sparser than the original. Very sparse matrices are easier to store and transmit than ordinary matrices of the same size. This is because the sparse matrices can be specified in the data file by providing locations and values of their non-zero entries.

It can be seen that in the final transformed matrix (after the specified level of decomposition, such as one level of decomposition (in our example above), we find many entries are zero. From this transformed matrix, the original matrix can be easily calculated just by the reverse operation of averaging and differencing i.e. the original image can be reconstructed from the transformed image without the loss of information (i.e. it yields a lossless compression). However, we need to achieve a higher degree of compression, so we have to consider lossy compression that will give us high compression ratio with reasonable (application specific) distortion amount.

In this case, a nonnegative threshold value say ε is set. Then any detail coefficient in the transformed data whose magnitude is less than or equal to ε is set to zero. It will increase the number of zeros in the transformed matrix and thus the level of compression will be increased. So, $\varepsilon = 0$ would be used for a lossless compression. If a lossy compression is used, an approximation of the original image can be constructed with some reasonable loss of image fidelity (depending on the value of ε). The setting of the threshold value is very important as there is a trade-off between the value of ε and the quality of the compressed image. The different thresholding methods we have used are: *hard thresholding* and *soft thresholding*. *Note:* for our experimental set up, we used hard thresholding and the thresholding is not applied on the approximate coefficient. These thresholding methods are defined as follows:

Hard Thresholding:

$$T(\varepsilon, x) = \begin{cases} 0, & \text{if } |x| < \varepsilon \\ x, & \text{otherwise} \end{cases} \tag{6.2}$$

Soft Thresholding:

$$T(\varepsilon, x) = \begin{cases} 0, & \text{if } |x| < \varepsilon \\ \text{sgn}(x)(|x| - \varepsilon), & \text{otherwise} \end{cases} \tag{6.3}$$

Note: For our experiment we used only hard thresholding for faster and energy efficient execution, and the threshold is applied only on the detail coefficients (H, V and D sub coefficients in the coefficient matrix). Also result of *global thresholding* where a single threshold value (such as 20 in our experiment above) is used for all levels (H,V and D),[1] and *level dependent thresholding* where level and orientation dependent thresholding is used. For example, a threshold value of 17 is used for H, and 22 for D.

6.2.4 Procedures and Experimental Results

Multi-resolution, is concerned with the representation and analysis of images at more than one resolution. For a *Multi-Resolution Analysis (MRA)*, a scaling function is used to create a series of functions called wavelets of an image, each differing by a factor of 2 from its nearest neighboring approximations. The resulting filtered output are *approximation*(A), *vertical*(V), *horizontal*(H) and *diagonal*(D) details of the image. In this experiment we will be using *Haar basis functions* described in the previous section. The Haar transform itself is both separable and symmetric and can be expressed in matrix form [24]:

$$T = HFH \tag{6.4}$$

where F is an $N \times N$ image, H is an $N \times N$ transformation matrix and T is the resulting $N \times N$ transform. For the Haar transform, the transformation matrix H contains the Haar basis functions, $h_k(z)$ for $k = 0, 1, 2, ..., N - 1$. The 2-dimensional DWT of function $f(x, y)$ of size $M \times N$ is given by [24]:

[1]Here *approximation*(A), *vertical*(V), *horizontal*(H) and *diagonal*(D) details of the image.

$$W^{A}_{(m,n)} = \frac{1}{\sqrt{MN}} \sum_{x=0}^{M-1} \sum_{y=0}^{N-1} f_{(x,y)} h^{A}_{(x,y)} \tag{6.5}$$

where $W^{A}_{(m,n)}$ is the approximation image and $h^{A}_{(x,y)}$ is the approximation coefficient.

$$W^{i}_{(m,n)} = \frac{1}{\sqrt{MN}} \sum_{x=0}^{M-1} \sum_{y=0}^{N-1} f_{(x,y)} h^{i}_{(x,y)} \tag{6.6}$$

where $i = \{H, V, D\}$ and $h^{i}_{(x,y)}$ are the horizontal, vertical and diagonal coefficients.

6.2.5 Energy Efficient Local Processing Using DWT

Unlike a wired system where unlimited processing can be performed with no power constraint, a wireless sensor (which is energy constrained) energy efficient signal processing is needed to maximize the lifetime of the network. In a wireless sensor network, communication is awkward and has a significant amount of power consumption. When the distance between the sensors and between the sensors and the base station increases, the energy spent in reliably transmitting data becomes costly. As discussed in literature [28, 35, 36] that communication is the most power consuming operation in wireless sensors, and the problem will be more exaggerated when the data is image or video data (very large in size).

In our work here, we are providing an energy efficient technique that will trade computation for communication as communication consumes more energy than computation [28]. We are using multi-resolution image processing technique (DWT, with *Haar filter*), and transmitting the approximate coefficient and re-transmit more refinement bits if the quality of the reconstructed image is below required by the application.

Steps/Algorithms

Step 1: Image acquisition by the sensor; upon external trigger by motion sensor, the sensor starts acquiring image data $I(m, n)$. Where $I_{curr}(m, n)$ is the current image

(image acquired by the sensor) and $I_{ref}(m,n)$ is the reference image (image previously transmitted by the sensor, temporal ...)

Step 2: Partition the image in to different macro-block sizes (each macro-block size is $1/4th$ of the original image).

Step 3: Compute the Mean Absolute Difference (MAD) of each sub-partitioned image of I_{curr} against I_{ref}.

The image is divided in to 4 macro-blocks and each macro-blocks is assigned LT (left top), RT (right top), LB (left bottom), and RB (right bottom).

$$\text{MAD}(I^{LT}_{curr}, I^{,LT}_{ref}) = \frac{1}{4mn}\sum_{x=0}^{m/2}\sum_{y=0}^{n/2}|I^{LT}_{curr}(x,y) - I^{LT}_{ref}(x,y)| \tag{6.7}$$

$$\text{MAD}(I^{RT}_{curr}, I^{RT}_{ref}) = \frac{1}{4mn}\sum_{x=m/2}^{m}\sum_{y=0}^{n/2}|I^{RT}_{curr}(x,y) - I^{RT}_{ref}(x,y)| \tag{6.8}$$

$$\text{MAD}(I^{LB}_{curr}, I^{LB}_{ref}) = \frac{1}{4mn}\sum_{x=0}^{m/2}\sum_{y=n/2}^{n}|I^{LB}_{curr}(x,y) - I^{LB}_{ref}(x,y)| \tag{6.9}$$

$$\text{MAD}(I^{RB}_{curr}, I^{RB}_{ref}) = \frac{1}{4mn}\sum_{x=m/2}^{m}\sum_{y=n/2}^{n}|I^{RB}_{curr}(x,y) - I^{RB}_{ref}(x,y)| \tag{6.10}$$

Step 4: Decide which partition (macro-block) to process further using DWT and hop it to the next sensor on the route towards the base station. Buffer the partition (sub-image) to $I_{buff}(x,y)$ for further processing.

Step 5: Perform a L level of decomposition DWT corresponding to resolution s. Based on the Haar wavelet filter coefficients discussed in Section 6.2, obtain the A(approximate), H(horizontal), V(vertical) and D(diagonal) sub-image coefficients and transmit the approximate detail(A).

$$W^{LL}(x,y) = \frac{1}{2s}[I_{buff}(sx,sy)+I_{buff}(sx+1,sy)+I_{buff}(sx,sy+1)+I_{buff}(sx+1,sy+1)]$$

$$W^{HL}(x,y) = \frac{1}{2s}[I_{buff}(sx,sy)+I_{buff}(sx+1,sy)-I_{buff}(sx,sy+1)-I_{buff}(sx+1,sy+1)]$$

$$W^{LH}(x,y) = \frac{1}{2s}[-I_{buff}(sx,sy)-I_{buff}(sx+1,sy)+I_{buff}(sx,sy+1)+I_{buff}(sx+1,sy+1)]$$

$$W^{HH}(x,y) = \frac{1}{2s}[I_{buff}(sx,sy)-I_{buff}(sx+1,sy)-I_{buff}(sx,sy+1)+I_{buff}(sx+1,sy+1)]$$

where $W^{LL}(x,y) = A$, $W^{HL}(x,y) = H$, $W^{LH}(x,y) = \mathrm{V}$, $W^{HH}(x,y) = D$ details of sub-image $I_{buff}(x,y)$.

Theoretical Analysis: Computation vs. Communication

In *Step 3*, MAD is calculated by pixel subtraction between the current I_{curr} and reference I_{ref} images and adding cumulatively. This requires $2n^2$ operations (n^2 operation for subtraction and n^2 operation for addition). This is the computation cost for the DWT using *Haar filter* depends on the requested resolution. At resolution 1 (scale, $s = 1$), according to *step 5* of the above algorithm, we have to perform $4n^2$ additions and subtraction to compute approximate(A), horizontal(H), vertical(V) and diagonal(D) details of the image acquired by the sensor. For more resolutions ($s > 1$), we have to perform DWT and repeat the transform recursively but only on the approximate(A) coefficients. So for resolution ($s = 2$), $4n^2$ operations for $s = 1$ and $\frac{1}{4}(4n^2)$ for $s = 2$, totally $4n^2 + n^2$ operations (add/sub). A similar procedure is executed for more resolution.

Table 6.1: Computation cost, DWT (Haar filter)

Type of Operation	Computation Cost(inst.)	Operations
Variance Computation	$2n^2$	sub,add
DWT(Haar, at $s = 1$)	$4n^2$	add,sub
DWT(Haar, at $s = 2$)	$4n^2 + n^2$	add,sub
DWT(Haar, at $s = 3$)	$4n^2 + n^2 + n^2/4$	add,sub

For communication cost, the sensors get resolution information from the base station and perform $DWT(HaarFilter)$ with the requested resolution. For example for $s = 1$, only $\frac{1}{4}(n^2)$ coefficients need to be sent to transmit the approximate coefficients.

For $s = 2$, the number of coefficients to transmit will be $\frac{1}{16}(n^2)$. Generally if a DWT is performed at resolution s, the number of approximate coefficients to be transmitted to the base station will be $\frac{1}{4^s}(n^2)$ bytes. The model for energy dissipation by the ra-

Table 6.2: Communication Cost, DWT (Haar Filter)

Type of Operation	Communication Cost(bytes)	Operations
Trans. Variance	–	-
Trans. Coeff. at $s = 1$	$n^2/4$	add,sub
Trans. Coeff. at $s = 2$	$n^2/16$	add,sub
Trans. Coeff. at $s = 3$	$n^2/64$	add,sub

dio module and communication module of the sensor when transmitting and receiving data is described in [25, 26, 28, 31]. We will use these models to compare computation cost and communication cost, and see the energy saving by trading computation for communication.

As described in [26], the radio module energy dissipation can be characterized into two types. The first is given by $E_{elec}(J/b)$, the energy dissipated to run the transmit or receive electronics and the second is given by $\varepsilon_{amp}(J/b/m^2)$, the energy dissipated by the transmit power amplifier to achieve an acceptable E_b/N_o at the receiver. We assume d^2 energy loss for transmission between sensors (assuming the distances between sensors are relatively short) [27]. To transmit a $k - bit$ packet a distance, d, the energy dissipated is:

$$E_{tx}(k, d) = E_{elec} \cdot k + \varepsilon_{amp} \cdot k \cdot d^2 \tag{6.11}$$

and to receive the $k - bit$ packet, the radio expends

$$E_{rx}(k) = E_{elec} \cdot k \tag{6.12}$$

For μAmp wireless sensor, $E_{elec} = 50nJ/b$ and $\varepsilon_{amp} = 100pJ/b/m^2$ [26]. To prolong the lifetime of the wireless sensor all aspects of the sensor system should be energy

efficient, there should be efficient network protocol layer and efficient signal processing algorithm. But our work here is mostly concerned about the energy dissipated at the radio and communication module since our work is on local energy efficient signal processing.

From Tables 6.1 and 6.4, we can compare communication vs. computation cost. As can be seen from the tables, the computation cost for DWT using Haar wavelets is dependent on the level of decomposition. For scale/decomposition level $s = 1$, $s = 2$ and $s = 3$, the computation cost is given as $4n^2$, $5n^2$ and $5.25n^2$ respectively, where n is the number of operations. For the same sequence of wavelet decomposition levels the communication cost is gives by $\frac{n^2}{4}$, $\frac{n^2}{16}$ and $\frac{n^2}{64}$ where n here is the number of bytes.
For $s = 1$, Computation cost $= 4n^2$ operations and Communication cost $= \frac{n^2}{4} \times 8$ bits.
For $s = 2$, Computation cost $= 5n^2$ operations and Communication cost $= \frac{n^2}{16} \times 8$ bits.
For $s = 3$, Computation cost $= 5.25n^2$ operations and Communication cost $= \frac{n^2}{64} \times 8$ bits.

Using the energy model in [31], the energy cost of transmitting 1000 bits a distance of 100 m is approximately the same as that for the executing 3 million instructions by 100 MIPS/W (million instruction per watt) processor. By this model, the energy spent for transmitting each bit over a distance of 100 m is sufficient enough to execute 3000 instructions. Based this, we can show how much savings we get by doing local processing on the sensors using DWT (Haar wavelets).
For s = 1, Computation cost $= 4n^2$ operations and Communication cost $= \frac{n^2}{4} \times 8$ bits. We are transmitting only a quarter of the original image size, which saves us $\frac{3}{4}$ of the size of the image (in bytes). So our saving will be: $\frac{3}{4}n^2 \times 8 = 6n^2$ bits. But this saving is at the expense of computing $4n^2$ operations. The energy expenditure for this operation is equivalent to $\frac{4}{3000}n^2$ bits using the same model in [31], the energy to transmit 1 bit is equal to energy spent to execute 3000 instructions.

$$\text{Net Saving(in bit, for s = 1)} = 6n^2 - \frac{4}{3000}n^2 \simeq 6n^2 \text{bits}$$

For s = 2, Following same procedure as above,

$$\text{Net Saving(in bit, for s = 2)} = 7.5n^2 - \frac{5}{3000}n^2 \simeq 7.5n^2\text{bits}$$

For s = 3,

$$\text{Net Saving(in bit, for s = 3)} = 31.5n^2 - \frac{5.25}{3000}n^2 \simeq 31.5n^2\text{bits}$$

Using this model we can compare computation cost vs. communication cost for $DWT(Haarfilter)$ for different resolution and show the saving by trading computation for communication.

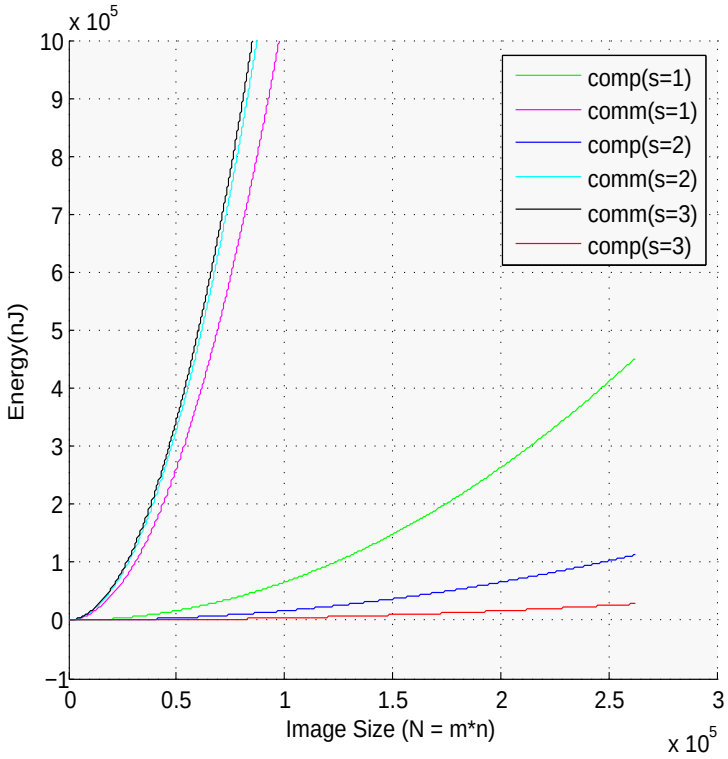

Fig. 6.3.: Computation vs. communication cost, DWT(s = 1,2,3)

Simulation: Computation vs. Communication

In the above section, theoretical analysis of *computation* vs. *communication* is provided. In this section, simulation results is provided. The simulation is done in Matlab (using wavelet toolbox).

A frame of size 320×240 is captured from a surveillance video "sanfrancisco_traffic.avi", a test sequence from UCLA Wireless Research and Development) and decomposed using 2 levels of DWT (Haar wavelet). The H, V and D position wavelet coefficients are thresholded using both global ($threshold = 20$) and level dependent thresholding ($threshold = 18, 20, 22$ for H,V and D, respectively).

Table 6.3: Simulation result, DWT (Haar filter, $L = 2$) with global and level dependent threshold

Metrics	Threshold: Global	Threshold: Level Dependent
MSE	0.164447	0.00585253
PSNR	55.97	70.46
Energy Retained	95.4%	98.0%
Null Coefficients	93.8%	93.8%
RLE Ratio	8.4115%	8.41%

As can be seen from Table 6.3, level dependent thresholding gives better energy retention of the original signal and better PSNR than global thresholding without affecting the compression ratio.

6.3 Background Subtraction Method for Image Compression

Background subtraction is a widely used approach for detecting moving objects from a static camera by differencing the current frame and a reference frame. The result highly depends on how the reference image (modeled background) represent the static scene (the scene with no moving object) of the camera view. So a good model for estimating the background is necessary for optimal result.

6.3.1 Background Model - Estimating Good Background

Several methods of performing background subtraction have been proposed in literature [67]. All these methods try to estimate the background model from the temporal sequence of the frames, each method with its benefits and limitations. In the next section, we provide some of these common techniques based on speed, memory requirement and accuracy.

6.3.2 The Most Common Approaches of Background Modeling

The approaches below range from simple approaches, aiming to maximize speed and limiting the memory requirement to more sophisticated approaches aiming to achieve the highest possible accuracy. Some of these are Running Gaussian Average, Temporal Median Filter, Gaussian Mixture Model, Kernel Density Estimation (KDE), Sequential KD Approximation, etc.

As discussed in Section 2.2.2, three common approaches are:

- Running Gaussian Average
- Temporal Median Filter
- Gaussian Mixture Model

6.3.3 Foreground Processing

The background for our model is created by using the Gaussian running average model, Equation (2.1) described in Section 2.2.2. The value for α in Equation (2.1) is set to 0.075 and a background is created using a static scene.

For each current frame, a foreground object (I_{fg}) is extracted/created by subtracting the background image (I^B) from the current frame (I^C) as follows.

$$I_{fg} = I^C - I^B \tag{6.13}$$

$$I^R = I_{fg} + I^B \tag{6.14}$$

If the frame is a 256 level grayscale, both the values of I_B and I_C ranges between 0 and 255 which requires 8 bits to encode each of the pixels. But the foreground image I_{fg} have values 511 distinct values between -255 to 255, which needs 9 bits to encode each value. We have proposed an algorithm to reduce the number of bits used to encode each pixel during Run Length Encoding in the next subsection.

6.3.4 Improving the Run Length Encoder

As we have noted the range of values in I_{fg} are -255 to +255. After applying a simple run-length encoding to the foreground, we transmit it as,

pixel run pixel run pixel run...

The goal of this encoding scheme is based on the assumption that the length of the byte stream should be much less than the original image since there is much redundant data (mostly zeros) in the foreground image.

Transmitting the Foreground Image, if the frame is a 256 level grayscale, both the values of I_B and I_C ranges from 0 to 255 which requires only 8 bits to encode each pixel. But the foreground image I_{fg} have 511 distinct values ranging between -255 and 255, which requires 9 bits to encode.

Most commercial sensors like *MCU(ATMEL 90LS8535)* and *TinyOS* comes with 8 bit cpu and store data in 8 bit chunk. An actual implementation that takes (for example) 8 bit input must store each 9 bit coefficient in a data type 16 bits wide, thus consuming twice the memory bandwidth.

Our Solution for this Problem, thresholding by dividing each pixel in the foreground image by an appropriate value. If we divide by two, we obtain $I_{fg}/2$,

which produces a range of values between -127 and 127 which is 255 distinct vales. Now 8 bits is required to encode this values. The maximum run now is 255. In this case each pixel value of the image is encoded as a pixel and run byte wise, e.g: $56, 56, 56, 56, 57, 125, 124, 124, 124$ is encoded as $56, 4, 57, 1, 125, 1, 124, 3$.

For example, if we divide the foreground by four, we obtain $I_{fg}/4$, which will make the range of values $[-63, 63]$, then adding the shift (64), we will have a range of values $[1, 127]$ which requires only 7 bits to encode. The eighth bit can be used as a flag bit to represent if that value is a pixel value or a run count (e.g. eighth bit equals 1 for pixel and zero for run count). Advantage of this scheme, in an 8 bit OS controller, we need only 7 bits to encode each pixel value of the foreground. Thus, the high bit can be used a flag to indicate if that value is a pixel or a run count. During decoding of the image the reverse operation has to be done to recover the correct values of the foreground pixel.

pixel pixel pixel run pixel run...

The maximum run now is 127. In this case the run will be counted bitwise, where the high bit is used as a flag to indicate if that byte is a pixel value or a run count.

If we divide the fore ground by 8, we obtain $I_{fg/8}$, will make the range of values between -32 and 32 which is 65 distinct vales and 6 bit is required to encode this values. It can be encoded as a 7 bit value plus a bit to flag if it is a pixel value or a run count. The maximum run now is 32.

Generally, if the divisor during quantization is greater than 4 and we view the byte as a bitstream, we can encode pixel with less bits.

- $D = 8$, needs only 7 bits (6 bits for pixel value and 1 bit for flag), $maxrun = 2^6$
- $D = 16$, needs only 6 bits (5 bits for pixel value and 1 bit for flag), $maxrun = 2^5$
- $D = 32$, needs only 5 bits (4 bits for pixel value and 1 bit for flag), $maxrun = 2^4$

$$I_Q = I_{fg}/D + Shift$$
$$I_R = D * (I_Q - Shift) + I_{bg}$$

where I_Q: is the quantized version of the foreground image (I_{fg}), I_R: is the reconstructed image, D: is the divisor.

Table 6.4: Encoding foreground image based on 10 neighboring images

Divisor	Shift	No. of bits to encode	Avg. PSNR	Avg. RLE
4	64	8	46.47	78.53
8	32	7	37.95	44.2
16	16	6	32.31	30.76

6.4 Exploiting Data Correlation Between Neighborhood Sensors for Energy Efficient Data Transmission in WMSN

High spatial density of sensor networks induces a high level of network data redundancy, where spatially proximate sensor readings are highly *correlated*. The sensor nodes can compress their data based on the fact that there is another sensor measuring data that is correlated with it. In video coding, several types of interframe predictions have been used to reduce the interframe redundancy. Motion compensated prediction has been used as an efficient scheme for temporal prediction. Likely, in here we propose a *Block Matching Algorithm (BMA)* method to fully exploit the spatial correlations that exist between sensor readings. Different from the conventional motion estimation, the proposed Block Matching Algorithm (BMA) will be executed on the decoder side to share complexity between encoder node and decoder (base station, with sufficiently enough power and computational resource). In this section we present an algorithm on how to exploit the correlation between sensors

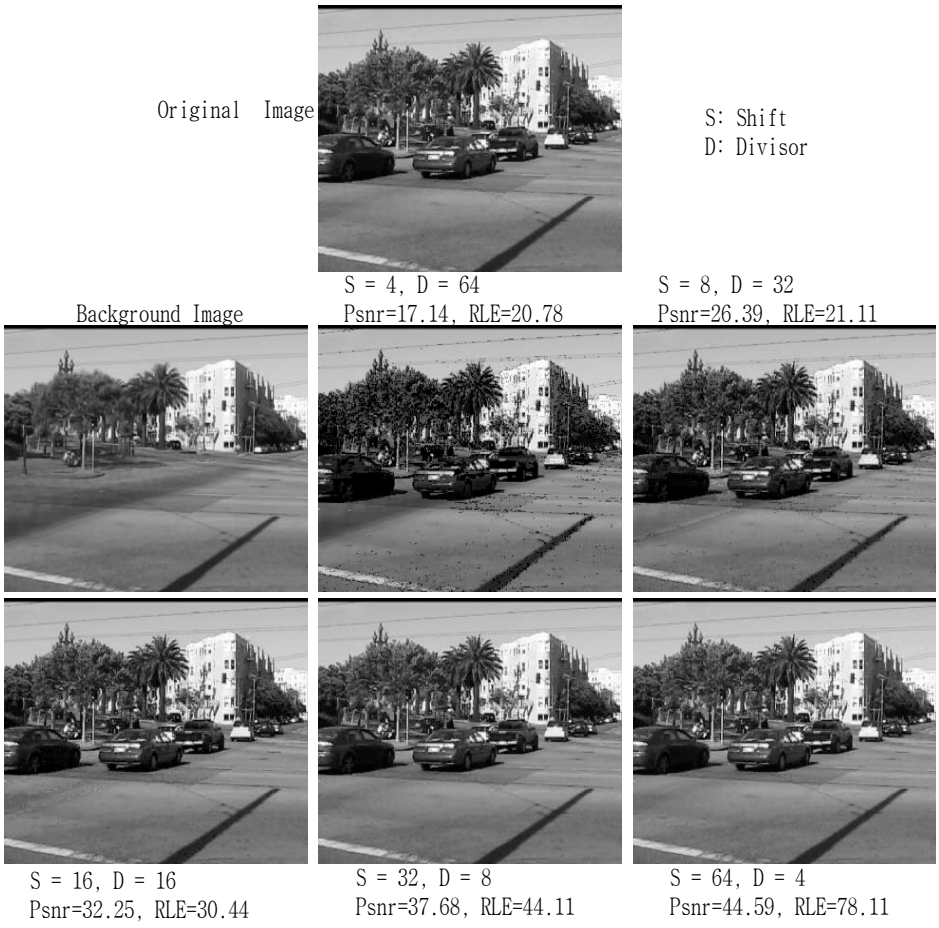

Fig. 6.4.: Run length encoding, with different divisor (threshold)

using Block Matching Algorithm (BMA). The correlation degree between sensors is determined by the overlapping sensing area of correlated nodes. We consider a $2D$ model for the sensing area of image sensors illustrated by Fig.6.5. Here Sensor A and Sensor B are within the same sensing radius, we denote R as the sensing radius. As can be seen from the figure, the sensing area of the two sensors overlap and hence redundant data will be collected by the two sensors.

At first each sensor compresses their reading and transmits it to the base station through the forward channel. Receiving the data, the base station computes and checks each pair of spatially close sensors to see if their data is highly correlated to exploit the correlation (correlation due to overlap of data between sensor measure-

ments who are close to each other). This can be achieved by using some metric to measure the correlation between sensor data's like block matching algorithm based on Mean-Absolute Difference (MAD).

6.4.1 Block Matching Algorithm

Consider an image divided into small non-overlapping blocks (such as 16×16). For each block in the first image the algorithm tries to find a block of the same size in the second image that is most similar to the block in the first image within a suitably sized search range. Different metrics can be used to measure similarity Such as computing the difference between blocks and use cross correlation, squared difference, absolute difference, etc. In our experiment, the metric used for matching the macro blocks is mean absolute difference (MAD), a small MAD implies macro blocks are similar (with some threshold).

$$MAD(A, B) = \frac{1}{m \cdot n} \sum_{p=1}^{m} \sum_{q=1}^{n} [A(p, q) - B(p, q)] \tag{6.15}$$

The function searches in the neighborhood of some given point in the second image by moving points in the block by the same offset. The search range and how we measure similarity has a great effect on the block matching algorithm, i.e. wider search range will result in the best match but at the expense of computation, and the threshold determines how similar the two macro-blocks are. A fairly low threshold has to be set to get less distortion in the reconstructed image since those blocks who are discovered "matched" by the algorithm will not be encoded again, rather they will be appended from the previously decoded block from the neighbor's measurement.

6.4.2 Transmission of Data After Receiving Codebook: Encoder Side

Once a codebook is created for a pair of sensors (group of sensors), the Base Station will broadcast the codebook along with the sensor id (each sensor has id and know its neighbors, this is set up during network discovery [68]). If sensor A and

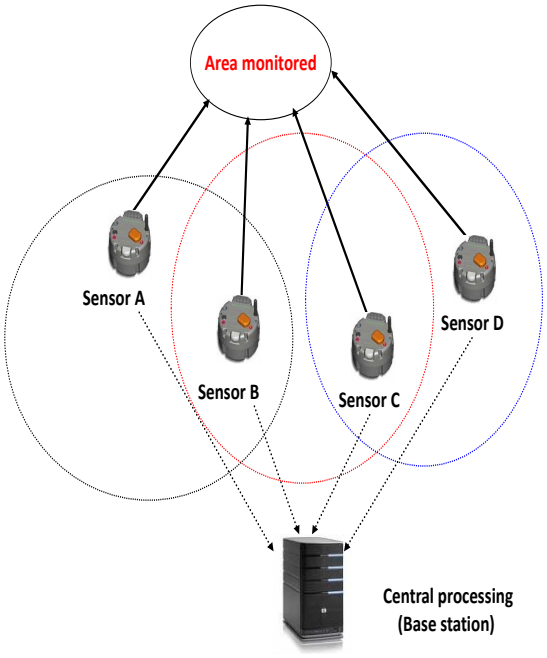

Fig. 6.5.: Overlap between proximate sensor measurement

sensor B have a codebook relationship as in Fig 6.4.1, then sensor B knows which blocks it needs to transmit and which blocks from sensor A can be used by the Base Station to reconstruct B's image. Thus sensor B, only needs to transmit those blocks that are not in the codebook.

Simulation Results Concerning Codebook

In this experiment we are testing our proposed algorithm of exploiting the spatial correlation between reading of proximate sensors. The experiment is conducted on the "san francisco_traffic.avi" video. Different sets of images are created from this video sequence, where each pair of image share some common image (150 out of 225 macroblocks, 16×16 sized macro blocks were used in the experiment).

Experiment:

Each pair of image (frame) is partitioned into blocks of 16×16, and a Block matching algorithm will be run on each pair of images to exploit the overlap area and those blocks within the pair are found to be *matched* if their MAD are within the given threshold, these blocks will then be flagged.

There are different factors affecting the efficiency of the codebook method. Some of these are, the choice of threshold, the choice of the number of frames used to build the codebook, etc.

Choosing an appropriate threshold is vital for getting an efficient codebook with minimal false positives. The higher the threshold, the more the probability that a false match will occur. The number of frames used to create the codebook will also affect how good the codebook will be. The more frames we used to create the codebook, the less the number of matched blocks will be since we are using all or none approach (i.e.: on a specific macro block all the frames used to compute the codebook has to agree that it is a match, else it will not be added in the codebook). Table 6.5 shows the creation of codebook using different threshold and different frames.

Analyzing the results in Table 6.5, as stated above the two images are created so that they have overlap of 150 macroblocks out of the total 225 macro block in each frame. With 0 thresholding and a single frame to create the codebook we have retrieved all the overlapped macroblocks (look at first row of Table 6.5), but with same threshold and 5 frames to create the codebook we have lost only a single macro block due to a false positive (row 4 of Table 6.5), and same result for with 0 threshold and 10 frames to create the codebook, all with a very good PSNR value. With $threshold = 3$ and a single frame to create the codebook, we have 198 macroblocks matched, which is higher than the total overlapped macroblocks between the two frames, this implies there are many false matches and the quality of the reconstructed image is expected to degrade ($psnr = 19.02$, row 2 of Table 6.5). With 5 frames to create the codebook, the number of matched macroblocks drops dramatically from 198 to 3, this saving

(which has only 3 macro block) is insignificant and the psnr is expected to be very high ($psnr = INF$(infinity)), and same result using 10 macroblocks to create the codebook. With $threshold = 9$ and a single frame to create the codebook, we have 216 matched macroblocks, lot of false matches and hence degraded reconstructed frame ($psnr = 14.90$). With 5 and 10 frames to create the codebook, only a single macro block match is found and the reconstructed image is of almost same quality as the original ($psnr = INF$).

From Table 6.5 and the analysis in the above paragraph, it can be deduced that the threshold and number of frames used to create the codebook has to be chosen carefully to get a good saving by using the codebook method. In our experiment, the results in row 4 and 7 in Table 6.5 have optimal values.

(a) Original Image

(b) Thresh = 0, Frame = 1, Match = 150

Fig. 6.6.: Reference image vs. frame with threshold = 0

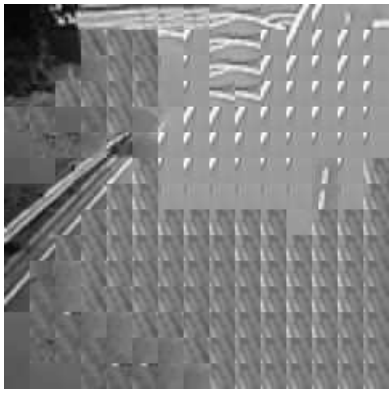

(a) Thresh = 3, Frame = 1, Match = 198

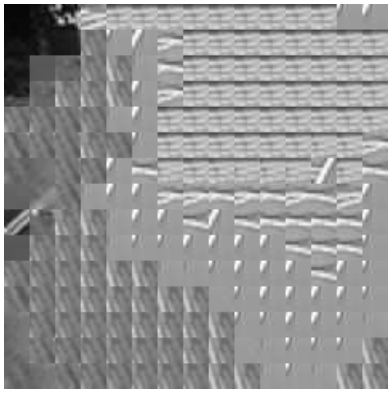

(b) Thresh = 9, Frame = 1, Match = 216

Fig. 6.7.: Frame with threshold = 3 vs. frame with threshold = 9

(a) Thresh = 0, Frame = 5, Match = 149

(b) Thresh = 3, Frame = 5, Match = 3

Fig. 6.8.: Frame with threshold = 0 vs. frame with threshold = 3

6.4.3 The Overall Encoding Process

The encoding system operates by switching modes between background subtraction method, Discrete wavelet transform and Codebook method based on optimizing feedback received from the decoder. We could use solely the DWT as the only encoding tool, but it is computationally more intensive than simple background subtraction method and/or codebook method. The background subtraction method is also not always efficient to be used as the only encoding system due to the difficulty of finding

(a) Thresh = 9, Frame = 5, Match = 1

(b) Thresh = 0, Frame = 10, Match = 149

Fig. 6.9.: Frame with threshold = 9 vs. frame with threshold = 0

(a) Thresh = 3, Frame = 10, Match = 3

(b) Thresh = 9, Frame = 10, Match = 1

Fig. 6.10.: Frame with threshold = 3 vs. frame with threshold = 9

a good background that stays same for long time (the background can be changing frequently due to illumination change and other external factors). The codebook method may not exist because suitable overlap between sensors may not exist. But observe we could use background subtraction or the DWT on the missing blocks, thus codebook should be the optimal method, when a good overlap exists.

By combining the advantages of all the encoding schemes, we can optimize the encoding system for better efficiency. For example, at first the DWT method can be used to encode the captured frames and the background model can also be run in

parallel to reconstruct a good representative background for each node. Once a good background is created, the encoding mode can be switched to background subtraction method[2].

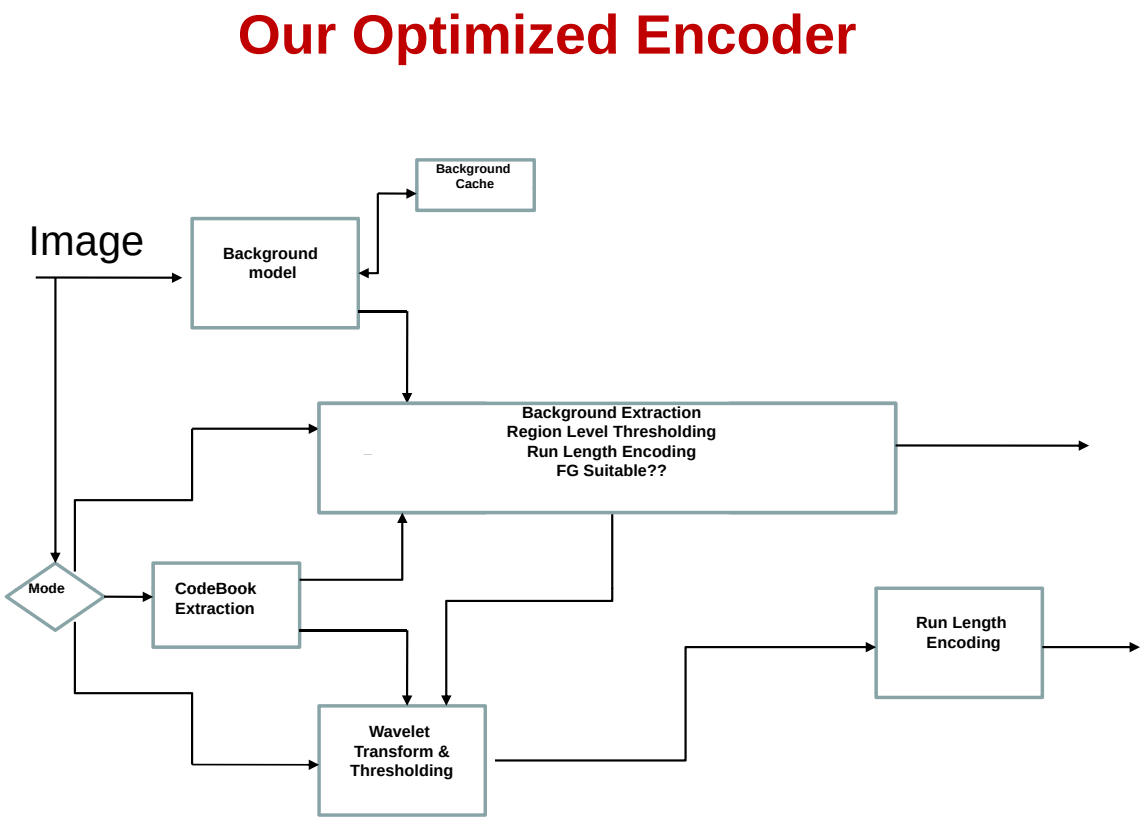

Fig. 6.11.: Encoding System

As can be seen in Fig.6.11, once a good representative background is made, the background cache will turn the flag on and encoding mode will be switched to background subtraction since it is computationally less intensive than DWT. Using this encoding technique a foreground object will be segmented and encoded using RLE to be transmitted to the base station. But before transmission, the decision box in Fig.6.11 will determine if the foreground is suitable, if not there must have been a dynamic change in the background of the scene and encoding mode will be switched

[2]Assuming a static node, each node will have a static background

Table 6.5: Simulation Result: Number of matched blocks between two frames, with different threshold

Threshold	No. of frames used To compute codebook	Number of hits out of 225	PSNR
0	1	150	68.92
3	1	198	19.02
9	1	216	14.90
0	5	149	INF
3	5	3	INF
9	5	1	INF
0	10	149	INF
3	10	3	INF
9	10	1	INF

to DWT and the background model will run in parallel again to create a good background representing the static scene. Different simulation results on these encoding schemes can be found in Chapter 7.

7. IMAGE QUALITY ASSESSMENT BY BASE STATION

7.1 Introduction

As described in Chapter 6, upon receiving the compressed signal from the sensors, the base station need to decode and reconstruct the image. Once the image is reconstructed the quality of the reconstructed signal has to be evaluated and the information has to be transmitted back to the encoding system through the backward channel. First for requesting re-transmission of the previous signal if the quality of the reconstructed signal is below the quality required by the application, and second to optimize algorithms and parameter settings of the encoding system.

Many efficient techniques have been developed to evaluate the quality of the reconstructed image for both lossless or lossy type of compression. The evaluation technique for lossless type of compression is straight forward since there will not be loss of information during the encoding process. The algorithm will be evaluated based on compression ratio, how fast the encoding process will be executed to be applied for real time applications and so on. Such an evaluation is outside the scope of the base station's concerns. Furthermore the compression techniques that we are implementing are certainly lossy. For lossy compression techniques the major problem in evaluating them, is the difficulty in type and amount of degradation in the reconstructed image.

Since the main objective of our work is on energy efficient image and video processing and transmission in wireless sensor networks, we won't be able to send more information about the original signal besides its compressed version. The only information available in the base station side is information from the reconstructed image; i.e. the decoder won't be able to use the common image quality assessment tools to

give feedback to the encoding system or to optimize the parameters in the encoding algorithm.

7.2 Image Quality Assessment Tools

Objective image and video quality metrics can be classified in to three broad categories based on the availability of the original image and video signal [73]:

Full-Reference (FR) QA methods, in which the QA algorithm has access to a *perfect version* of the image or video against which it can compare a *distorted version*. The *perfect version* generally comes from a high-quality acquisition device, before it is distorted by compression artifacts and transmission errors. However, the reference image or video generally requires much more resources than the distorted version, and hence FR QA is generally only used as a tool for designing image and video processing algorithms for in-lab testing, and cannot be deployed as an application.

Currently the most widely used objective image and video fidelity (distortion) metrics are Mean Square Error (MSE) and Peak Signal to Noise Ration (PSNR).

$$MSE = \frac{1}{N}\sum_{i=1}^{N}(x_i - y_i)^2 \tag{7.1}$$

$$PSNR = 10\log_{10}\frac{L^2}{MSE} \tag{7.2}$$

where N is the number of pixels in the image or video signal, and x_i and y_i are the i^{th} pixel in the original and distorted signals respectively. L is the dynamic range of the pixel (for an 8 bits per pixel monotonic signal L is equal to 255).

An objective image and video quality measure metric that is commonly used is the Structural Similarity Index (SSIM) [18]. It is a full reference metric, i.e. it measures image quality based on an initial uncompressed or distortion-free image as reference. SSIM is designed to improve on traditional methods like peak signal-to-noise ratio (PSNR) and mean squared error (MSE), which have proved to be inconsistent with human eye perception.

The SSIM metric is calculated on various windows of an image. The measure between two windows x and y of common size $N \times N$ is:

$$SSIM(x,y) = \frac{(2\mu_x\mu_y + c_1)(2\sigma_{xy} + c_2)}{(\mu_x^2 + \mu_y^2 + c_1)(\sigma_x^2 + \sigma_y^2 + c_2)} \tag{7.3}$$

where, μ_x is the average of x, μ_y is the average of y, σ_x^2 is the variance of x, σ_y^2 is the variance of y, σ_{xy} is the covariance of x and y, $c_1 = (k_1 L)^2$, $c_2 = (k_2 L)^2$ two variables to stabilize the division with weak denominator, L is the *dynamic range* of the pixel values (typically $2^{w_0} - 1$, where w_0 is the number of bits per pixel), and $k_1 = 0.01$ and $k_2 = 0.03$ by default. Example of images comparing MSE, PSNR and SSIM is

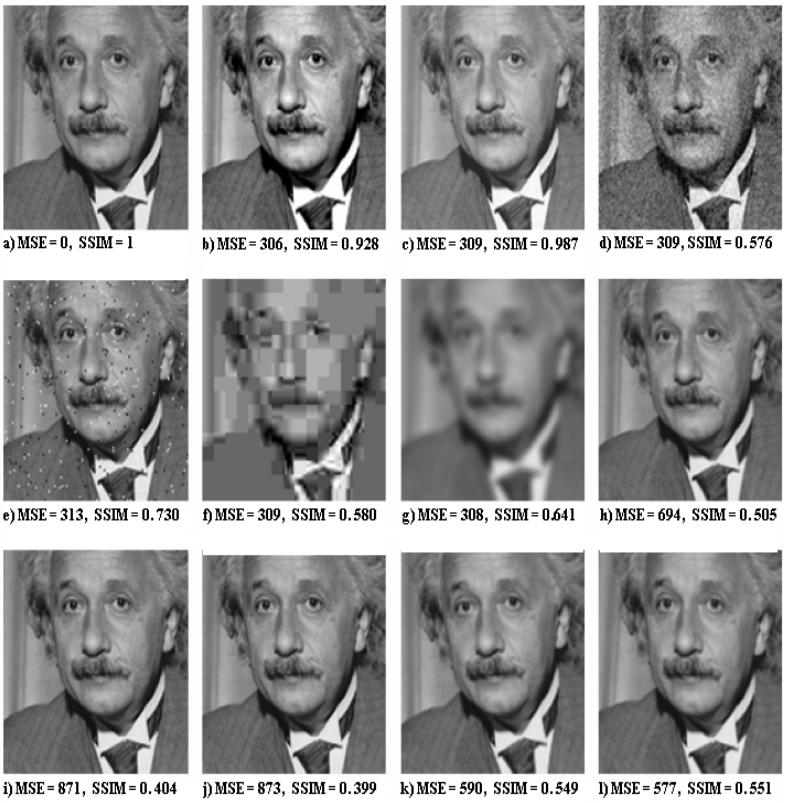

Fig. 7.1.: Comparison of image similarity metrics among MSE, PSNR and SSIM

given in Fig.7.1. The problem with this approach is that it requires the covariance and so both the reference image and the reconstructed image is needed.

No-Reference (NR) QA methods, in which the QA algorithm has access only to the distorted signal and must estimate the quality of the signal without any knowledge of the *perfect version*. Since NR methods do not require any reference information, they can be used in any application where a quality measurement is required. However, the price paid for this flexibility is in terms of the ability of the algorithm to make accurate quality predictions, or a limited scope of the NR QA algorithm (such as NR QA for JPEG images only etc.).

Although this type of image and video quality assessment tool is very efficient for our research to optimize the encoding system with out sending side information to the station, there is no general metric available to accurately measure the similarity between two images with out having the original (or some side information about the original) image or video at the base station (decoder) side. Several NR quality assessment applications have been addressed in [73] and [19].

Reduced-Reference (RR) QA methods, in which partial information regarding the "perfect version" is available. A side-channel (called an RR channel) exists through which some information regarding the reference can be made available to the QA algorithm. RR QA algorithms use this partial reference information to judge the quality of the distorted signal.

Our work uses Reduced-Reference (RR) QA method, where some side information besides the compressed version of the image is sent to the decoder (base station) using the side channel.

7.3 Reduced-Reference (RR) QA Methods, Our Approach (Technique)

In our approach we considered three different metrics that the Base Station could use to evaluate the quality of the reconstructed image at the base station. These are *Thumbnail PSNR*, *Mean test* and *Variance test*.

7.3.1 Thumbnail

An image thumbnail is produced after the partitioning of an image into quadrilateral shape (usually square) blocks of pixels, and constructing a thumbnail image comprising blocks, of single pixel-size, of uniform pixel value. The blocks in the thumbnail are uniformly scaled with respect to those of the image.

The image will be partitioned in to constant sized blocks each of row r and column c, $B[r][c]$. The mean of each macro block μB_i is given by:

$$\mu_{B_i} = \frac{\sum_{p=1}^{r}\sum_{q=1}^{c} B_i(p,q)}{r \cdot c} \tag{7.4}$$

where,

- μ_{B_i} : is mean of macro block i (where $i = 1, \ldots, n_o$)
- n_0: number of macro blocks. For an image of size $M \times N$ and macro block size $m \times n$, the number of macro blocks n_0 is given by:

$$n_0 = \frac{M}{N} \cdot \frac{m}{n}$$

7.3.2 Evaluating Thumbnail Image Quality

The thumbnail image is based on single pixels representing each macro blocks of the original image. So it contains one pixel of gray-scale to represent the block $B[r][c]$.

We use the thumbnail of the original image as a reference image. The thumbnail image is created from the original image using the procedure discussed in Section 7.3.1 and transmitted as a side information using the communication channel to the Base Station (decoder).

Let X and Y be two random variables mapping PSNR of reference image vs. reconstructed image, and their thumbnail version. The joint behavior of X and Y is fully captured in the joint probability distribution. For a continuous distribution

$$E(X^m Y^n) = \int \int_{\infty}^{-\infty} x^m y^n f_{xy}(x,y) dx dy \tag{7.5}$$

Fig. 7.2.: 256×256 8-bit grayscale girls image with mean thumb image based on 4×4 blocking.

For discrete distributions, the joint behavior of X and Y is:

$$E(X^m Y^n) = \sum_{x \epsilon S_x} \sum_{y \epsilon S_y} x^m y^n P(x, y) \tag{7.6}$$

The covariance function is a number that measures the common variation of X and Y. It is defined as

$$cov(X, Y) = E[(X - E[X])(Y - E[Y])] \tag{7.7}$$

The covariance is determined by the difference in $E[XY]$ and $E[X]E[Y]$. If X and Y are statistically independent then $E[XY]$ would equal $E[X]E[Y]$ and the covariance would be zero (but this will never happen when X and Y represent reconstructed image and original image). The correlation coefficient ρ can be produced by normalizing the covariance.

$$\rho = \frac{cov(X, Y)}{\sqrt{var(X)var(Y)}}. \tag{7.8}$$

Then ρ can be computed as

$$\rho = \frac{\sum_m \sum_n (A_{mn} - \bar{A})(B_{mn} - \bar{B})}{\sqrt{(\sum_m \sum_n ((A_{mn} - \bar{A})^2))(\sum_m \sum_n ((B_{mn} - \bar{B})^2))}} \tag{7.9}$$

where $\bar{A}$ is the mean of matrix A, and $\bar{B}$ is the mean of matrix B. The correlation coefficient is bounded by $-1 \leq \rho \leq 1$. It will have value $\rho = 0$ when the covariance is zero (when X and Y are statistically independent); and value $\rho = \pm 1$ when X and Y are perfectly correlated or anti-correlated respectively.

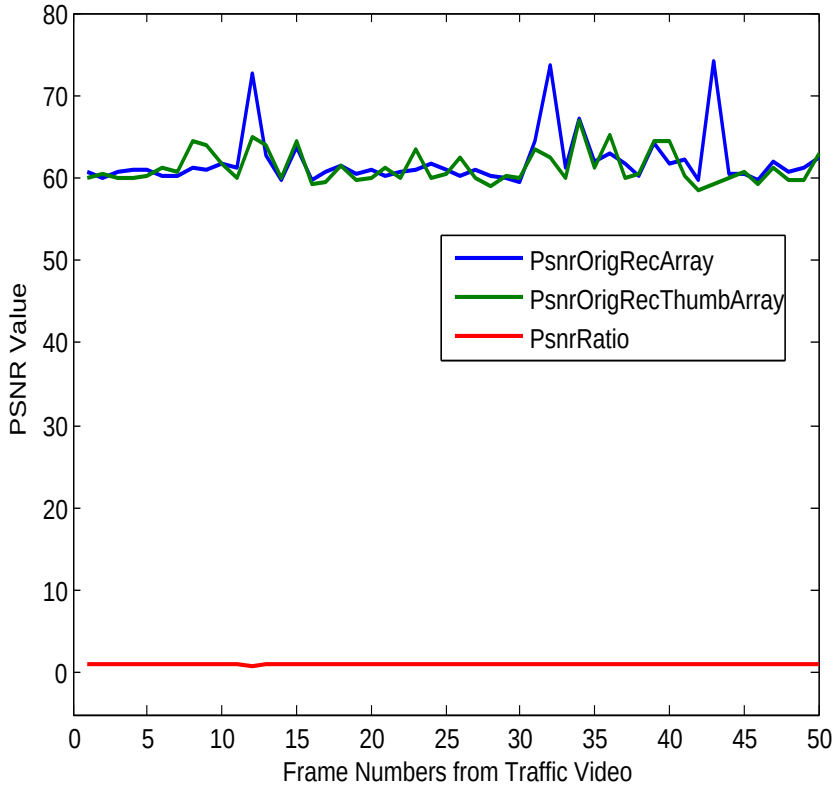

Fig. 7.3.: PSNR: Original-reconstructed vs. thumb version of Orig-rec

Is the Thumbnail Approach Sufficient to Assess the Quality at the Base Station?

Using the Thumbnail approach to assess quality of the reconstructed image in the Base Station is not sufficient to determine the quality of the reconstructed image at the Base Station. The following example illustrates the weakness of solely relying on the Thumbnail approach, when used alone to assess quality of the image.

(a) Bike *(b) Thumbnail of Bike*

Fig. 7.4.: Image: Bicycle and its thumbnail version

Clearly an average of a block can be preserved, yet the block may not be identical to the original block. In the following, we modified each block of the Bike Fig 7.4, so that the average of the block is the same as the average of the Girls image Fig. 7.5 by taking as many pixels from the Bike's block as possible, and then setting the remaining pixels to zero (black).

The conclusion that the ModBike Thumb and the Girl Thumb is similar is confirmed by examining the PSNR values in the following table.

As can be seen from Fig 7.6 and Table 7.1, the thumbnail PSNR identifies the image of ModBike as close to the Girl image. Hence transmitting the thumbnail version

(a) Girls

(b) Thumbnail of Girls

Fig. 7.5.: Image: Girls and its thumbnail version

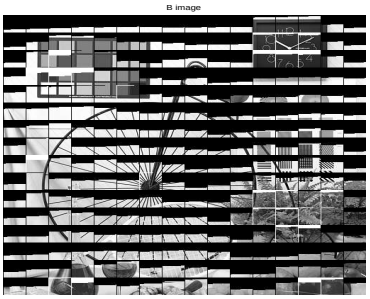

(a) ModBike

(b) Thumbnail of ModBike

Fig. 7.6.: Image: Bicycle modified and its thumbnail version

of the original image as the only reference to assess the quality of the reconstructed image will not always be accurate to assess that the original image and the reconstructed image are similar. For example, from Table 7.1, images G and B are two different/uncorrelated images with a PSNR value between them is 8.33, whereas their thumbnail versions have PSNR value of 37.75. So the proposed thumbnail method

Table 7.1: PSNR value of original image vs. thumbnail image

image1	image2	psnr val
Bike	ModBike	6.71
Bike Thumb	ModBike Thumb	7.13
G	H	6.50
Girl Thumb	ModBike Thumb	7.30
Girls	Bike	8.33
Girls Thumb	Bike Thumb	37.75

should not be used as the sole metric for assessing image quality, rather it has to be used in combination with other methods. We proposed using statistical tests along with the Thumbnail to provide quality assessment.

7.4 Statistical Test

A classical approach to determining if one has seen sufficient evidence to prove a claim is to use a statistical test. The idea is you have a hypothesis, and you would like to prove it is true (i.e. you have evidence that it is true). This is typically called the *alternative hypothesis*, denoted by H_a. The opposite of the alternative hypothesis is the null hypothesis, which is denoted by H_0. Typically when you construct the statistical test design, you assume that the null hypothesis is valid until you have evidence to the contrary. Your confidence level of your final conclusion is weighed by some probability, and from this you construct a rejection region. You then collect evidence and you compute a test statistic. If the test statistic falls in the rejection region then you have evidence that say the null hypothesis is false and you conclude the alternative hypothesis is true. If the test statistic lies outside the rejection region then you conclude the null hypothesis is true. Both the test statistic and the rejection region are dependent on the probability distribution you assume that the data collected fits.

7.4.1 Mean Test

In this test, on a block by block basis, we could test if the captured image is the same as the reconstructed image on average per block. The Base Station does not need the captured image, but rather it needs to know for each block from the captured image:

- how many pixels are in each block
- the sum of the pixel values (i.e. $\sum x_i$ where x_i is a pixel value ranging from 0 to 255)
- the sum of the squares of the pixel values (i.e. $\sum x_i^2$ where x_i is a pixel value ranging from 0 to 255)

If there are M blocks then we will need to transmit $2M + 1$, this would require $M \cdot$ size of unsigned int $+1$ bytes. We now describe how we apply the Mean test to assess the quality of the reconstructed image.

H_0 : *For block B: the average pixel in block B of the original image* $I_{Orig,B}$ *is the same as the average pixel in block B of the reconstructed image* $I_{Recon,B}$

H_a : *For block B: the average pixel in block B of the original image* $I_{Orig,B}$ *IS NOT THE SAME as the average pixel in block B of the reconstructed image* $I_{Recon,B}$

Test Statistic

$$z_* = \frac{\sum_{a_i \in I_{Orig,B}} a_i - \sum_{y_i \in I_{Recon,B}} y_i}{n \cdot S_{Orig}} \tag{7.10}$$

where $S^2_{Orig} = \frac{\sum_{a_i \in I_{Orig,B}} a_i^2 - \bar{a} \sum_{a_i \in I_{Orig,B}} a_i}{n-1}$ and n is the number of pixels in a block

Rejection Region

Reject H_0 provided $z_* \notin (-z_{.5+\alpha/2}, z_{.5+\alpha/2})$, otherwise accept H_0.

Here $z_{.5+\alpha/2}$ is the result of inputting $.5 + \alpha/2$ to the inverse of the CDF of the Gaussian (0,1) probability distribution. Because we are running this test backwards, we should set α to small nonnegative value like 0.01. This can be summarized in the following algorithm.

Algorithm 1 Mean test

1: Compute Rejection Region $\mathcal{R}_{meansig}$ based on *meansig*
2: **for** each block B **do**
3: Compute test statistic t_B
4: **if** test statistic $t_B \in \mathcal{R}_{meansig}$ **then**
5: Accept H_a, i.e. this block B of reconstructed image has a different mean then the for original image's block
6: **else**
7: Accept H_0, i.e. this block B of reconstructed image has the same mean as block B of the for original image

7.4.2 Variance Test

In this test, on a block by block basis, we could test if the variability of the captured (reference) image is the same as the variability of the reconstructed image. The Base Station does not need the captured image, but rather it needs to know for each block from the captured image:

- how many pixels are in each block
- the sum of the pixel values (i.e. $\sum x_i$ where x_i is a pixel value ranging from 0 to 255)

- the sum of the squares of the pixel values (i.e. $\sum x_i^2$ where x_i is a pixel value ranging from 0 to 255)

If there are M blocks then we will need to transmit $2M + 1$, this would require $2M \cdot$ size of unsigned int $+1$ bytes. However all the data that the sensor will need to transmit for the Mean test will already have been transmitted. Variance Test is as follows:

H_0 : *For block B: the variability in block B of the original image* $I_{Orig,B}$ *is the same as the variability in block B of the reconstructed image* $I_{Recon,B}$

H_a : *For block B: the variability in block B of the original image* $I_{Orig,B}$ *IS NOT THE SAME as the variability in block B of the reconstructed image* $I_{Recon,B}$

Test Statistic

$$f_* = \frac{S^2_{1,Orig}}{S^2_{2,Recon}} \tag{7.11}$$

where

$$S^2_{1,Orig} = \frac{\sum\limits_{a_i \in I_{Orig,B}} a_i^2 - \bar{a} \sum\limits_{a_i \in I_{Orig,B}} a_i}{n-1}$$

and

$$S^2_{2,Recon} = \frac{\sum\limits_{y_i \in I_{Recon,B}} y_i^2 - \bar{y} \sum\limits_{y_i \in I_{Recon,B}} y_i}{n-1}$$

Rejection Region Reject H_0 provided if either $f_* > FFR$ or $f_* < FFL$ otherwise accept H_0. Here FFL and FFR are dependent on the probability varsig, we used: FFR is the value or which the CDF of the F distribution with degrees of freedom $v_1 = n-1$ and $v_2 = n-1$ satisfies $Prob(F < FFR) = .5 + \frac{\text{varsig}}{2}$ and FFL is the value or which the CDF of the F distribution with degrees of freedom $v_1 = n-1$ and $v_2 = n-1$ satisfies $Prob(F < FFL) = .5 - \frac{\text{varsig}}{2}$

7.5 Applying Three Metrics for Quality Assessment

As discussed earlier, the base station needs to give each sensor feedback concerning the quality of the transmitted image after reconstruction. This can be done on a per transmission basis (which would be expensive from a transmission and receiving cost point of view) to some periodic request. The sensor has only the reconstructed image and it needs to have the original image to evaluate the quality of the reconstructed image. But it is counterproductive to send the original image to the decoder to assess the quality of the reconstructed image. We have decided to have the sensor transmit additional data as side information related to each macro block B_i of the original image, for $i = 1 \ldots, NumBlks$. The data transmitted for each are the sum of the pixels and the sum of the squares of the pixel values. With this data, the Base Station can construct the thumbnail $thumb_{orig}$ version of the original image, as well as the mean μ_{orig,B_i} and variance σ^2_{orig,B_i} for each macro block.
Thus, the Base station can:

1. Construct the thumbnail of the reconstructed Image $thumb_{Recon}$ and compute the PSNR of $thumb_{Orig}$ with $thumb_{Recon}$, if this value is not suitable the Base Station can ask for a retransmission of the image (under a different mode).

2. For each macro block B_i of the reconstructed image, for $i = 1, ..., NumBlks$, compute the mean $\bar{x}_{Recon,B_i}$ pixel value for that block and conduct a statistical mean test does $H_0 : \bar{x}_{Recon,B_i} = \mu_{Orig,B_i}$

   The test statistic is $t_{B_i} = \frac{\bar{x}_{Recon,B_i} - \mu_{Orig,B_i}}{\sigma_{Orig,B_i}}$

   Reject H_0: If the test statistic falls into the rejection region we reject H_0 and so the mean pixel values of the block are not equal. Consequently the transmitted image is not representative of the captured image in that block. As the Base Station has seen evidence that the images are not the same, they should ask for a retransmission of that block (not the whole image). Because this test is backwards, i.e. assumes the means are the same unless we find evidence they

are not, the rejection region should be "larger". Here we choose meanSig small (in our simulation it was 0.01). Let $t = \frac{meanSig}{2}$, and let $z_{0.5+t}$ denote the value such that the Gaussian with mean zero, variance one, and CDF $F(x)$ satisfies $F(z < z_{0.5+t}) = 0.5 + t$.

The rejection region consists of all z such that

$$z < -z_{0.5+t} \text{ OR } z > z_{0.5+t}$$

3. For each macro block B_i of the reconstructed image, for $i = 1, ..., NumBlk$, compute the variance s^2_{Recon,B_i} pixel value for that block and conduct a statistical variance test does $H_0 : s^2_{Recon,B_i} = \sigma^2_{Orig,B_i}$

   The test statistic is $f_* = \frac{\sigma^2_{Orig,B_i}}{s^2_{Recon,B_i}}$,

   Of course if the variability of the transmitted block and the variability of the block of the original image are identical, then the test statistic should be one. In general we would expect if the reconstructed image is close to the original, then for each block the test statistics should be close to 1. Thus using the F Distribution.

   Reject H_0 provided if either $f_* > FFR$ or $f_* < FFL$ other wise accept H_0. We used varsig = .2 so FFR is the value or which the CDF of the F distribution with degrees of freedom $v_1 = n-1$ and $v_2 = n-1$ satisfies $Prob(F < FFR) = .5+.1$ and FFL is the value or which the CDF of the F distribution with degrees of freedom $v_1 = n - 1$ and $v_2 = n - 1$ satisfies $Prob(F < FFL) = .5 - .1$

We conducted the following experiment. By looking at the *traffic.avi* video. We took a 240×320 video frame. We then partitioned this frame into two parts a left and a right, each 240×240. Thus there is a 240×150 intersection between the two. In our simulation, the macro block size was 16×16, so there are 225 total blocks, and between these two images (left and right), 150 of the blocks will be identical. We constructed a codebook using either one frame or five frames using the techniques described in Section 8.1.2. We selected threshold ranging from 0, 3, 9 and 12. After generating the

codebook based on number of frames (to build codebook) and threshold, we divided the remaining video into 24 equal sections and selected as a test frame the last frame of each sections, dividing it into a left and right part. Thus we had a total of 24 pairs of test images. We then ran the codebook scheme on each of the 24 test. We computed the averages of the PSNR, thumbnail PSNR, no. of blocks passing the mean test, and number of blocks passing the variance test. The results are presented in Table 7.2.

As can be seen from Table 7.2, for a single frames used to build the codebook, the number of matched macroblocks increses as the threshold increases. There are 150 macro blocks shared between the two frames and we discover that by using $threshold = 0$, but as the threshold increases from 0 to 3, 9, 12, the number of blocks matched increases from 150 to 209, 224, 225 respectively. This is because of the false matches between the macro blocks in the two frames within the given threshold. And the psnr value is seen degraded due to the false assessment indicators. To make up (refine) the false assessment indicators, we used mean and variance statistical test and it can be seen that the number of macro blocks that are accurate (those determined by the Base Station) decrease as the threshold increases, this is identified by the mean and variance test (see *no. of blocks passing variance test*) and of course much improved psnr.

Now assume that the Base Station requests a retransmission for each block B which failed the mean test, then the image that the Base Station will calculate is I'_{Recon}, which can be computed by Algorithm 2.

If the Base Station requires that a "good block" must pass both the mean test and the variance test then they would request a retransmission for each block B which fails the mean test or the variance test. Then the image that the Base Station will calculate is I''_{Recon}, which can be computed by Algorithm 3.

As can be seen from Table 7.3, the quality of the reconstructed image (after retranmssion) is highly improved when the Base Station requires blocks to pass both

Table 7.2: Codebook results on traffic.avi video

Threshold	No. (frames) to build Codebook	No. blocks in Codebook	PSNR	Thumbnail PSNR	No. (blocks) passing Mean Test	No. (blocks) passing Variance Test
0	1	150	Inf	Inf	225	225
3	1	209	15.598	19.936	69.958	74.5
9	1	224	13.24	17.288	23.458	28.541
12	1	225	12.165	15.780	15.750	20.041
9	5	35	39.333	44.9977	201.5	203.9

Algorithm 2 Computing I'_{Recon}

1: **for** each block B **do**
2: **if** $I_{Recon,B}$ with test statistic t_B passes *Mean Test* with rejection region $\mathcal{R}_{meansig}$ **then**
3: $I'_{Recon,B} = I_{Recon,B}$
4: **else**
5: $I'_{Recon,B} = I_{Orig,B}$

Algorithm 3 Quality assessment using both mean and variance test–computing I''_{Recon}

1: **for** each block B **do**
2: **if** $I_{Recon,B}$ with test statistic f_B passes *Variance Test* with rejection region $\mathcal{F}_{varsig}$ **then**
3: $I''_{Recon,B} = I'_{Recon,B}$
4: **else**
5: $I''_{Recon,B} = I_{Orig,B}$

Table 7.3: Estimating retransmission requests by base station

Threshold	No. frames to build Codebook	No. blocks in Codebook	PSNR of I'_{Recon}	PSNR of I''_{Recon}	No. Blocks passing variance test
0	1	150	INF	INF	225
3	1	209	40.14	48.39	75
9	1	224	32.69	37.30	28
12	1	225	36.38	48.36	20
9	5	35	47.39	48.01	213

the mean test and the variance statistical test. Of course this comes at the expense of bandwidth, since more blocks will need to be transmitted. There are 150 macro blocks shared between the frames taken in the test, but out of these only 75, 28, 20 macro blocks are matched after the variance test using only a single frames to create the codebook and threshold of 3, 9 and 12 respectively.

The result in Table 7.4 concerns image quality metrics for images compressed using integer based Haar DWT. For each macro block in the reconstructed image, we run the Mean test and if it doesn't pass then that macro block will have to be retransmitted. In our experiments, all the reconstructed images, even when applying different thresholds, had good psnr values, and the thumbnail image has a much better psnr then the full image, this is due to the fact that the thumbnail version is created by averaging each block and this averaging will suppress the noise introduced by during compression. Both the reconstructed image when computing I'_{Recon} and I''_{Recon} have good psnr but the number of macro blocks that have to be retransmitted increase with the threshold. Thus, a good threshold should be selected depending on the quality that the application requires.

From Table 7.5, we see that using the techniques described in Section 6.3.4, that the reconstructed images have decent psnr values for divisors of 4,8 and 16. Even a

Table 7.4: Wavelet transform-2 levels of decomposition

Threshold	PSNR	Thumbnail PSNR	No. (blocks) passing Mean test	PSNR of I'_{Recon}	PSNR of I''_{Recon}	No. (blocks) passing Variance Test
16	36.04	60.439	225	35.67	37.26	145
18	35.16	60.87	225	34.82	36.65	140
20	34.35	61.13	225	34.169	36.346	131
24	32.90	61.66	225	32.59	36.302	98

divisor equal to 32 has a psnr value at a level which could used in some applications. We can infer from Table 7.5 that the Mean test failed for almost every block, which would mean the Base Station would be required to retransmit almost all blocks. However the reconstructed images did well on the variance test. We then computed I'''_{Recon}, which consists of all block of the reconstructed image which pass the variance test. For those blocks that fail we use the original image. Table 7.6 shows the results. Here we see that we would not have to retransmit that many blocks (for example, for divisor equal to 8 we see 174 out of the 300 blocks pass). Even for a divisor equal to 32 we achieve a decent psnr and do not have to retransmit 45 blocks.

Algorithm 4 Quality Assessment using only Variance test – computing I'''_{Recon}

1: **for** each block B **do**
2: **if** $I_{Recon,B}$ with test statistic f_B passes *Variance Test* with rejection region $\mathcal{F}_{varsig}$ **then**
3: $I'''_{Recon,B} = I_{Recon,B}$
4: **else**
5: $I'''_{Recon,B} = I_{Orig,B}$

Table 7.5: Foreground - RLE with threshold (based on 10 images near background) 240×320 image (300 blocks)

Divisor	Avg	PSNR RLE	Thumbnail PSNR	No. (blocks) passing Mean test	PSNR of I'_{Recon}	PSNR of I''_{Recon}	No. passing Variance test
4	77.37	46.446	51.53	93.7	52.15	52.15	263
8	49.3	37.6	40.26	1.9	INF*	INF*	174
16	33.5	31.37	33.62	0.8	INF*	INF*	117
32	23.85	25.18	27.54	0.2	INF*	INF*	45
64	18.31	19.275	21.776	0	INF*	INF*	14

Table 7.6: RLE with threshold assessing by using only the variance test

Divisor	avg PSNR	PSNR of I'''_{Recon}	no. (blocks) passed
4	46.446	46.89	263
8	37.6	39.324	174
16	31.37	35.011	117
32	25.18	33.671	45
64	19.275	34.896	14

8. DECODER

We now discuss the decoder and decoding process. Recall that we have switched the traditional complex encoder/simple decoder to a simple encoder/complex decoder by placing some of the intensive computation on the decoder side (assuming the base station has enough computational resources).

8.1 Decoding Packets and Coordinating Sensor Operation

The primary function of the decoder is undoing the encoding so that the original information can be retrieved. As it discussed earlier, it is infeasible to use the existing state-of-the-art video coding algorithms such as *MPEG 2/4*, *H.264* etc to compress sensor readings due to their high computational complexity.

8.1.1 Decoding Packets Received from the Sensor:

The decoding procedure is such that it will decode the bit stream received and assimilate the data to retrieve the transmitted signal. The design of the decoder is based on the inverse operations of the technques discussed earlier. The decoder will appear a illustrated in Fig 8.1.

Decoding Packet Encoded using Background Subtraction Method

The decoder will read the packet header received from the sensors, and if the packet mode was encoded using the *Background Subtraction Method*, the decoder will perform the following operations to reconstruct the image. First update the background model:

$$I_{t+1}^{B} = \alpha I_{t}^{C} + (1 - \alpha) I_{t}^{B}.$$

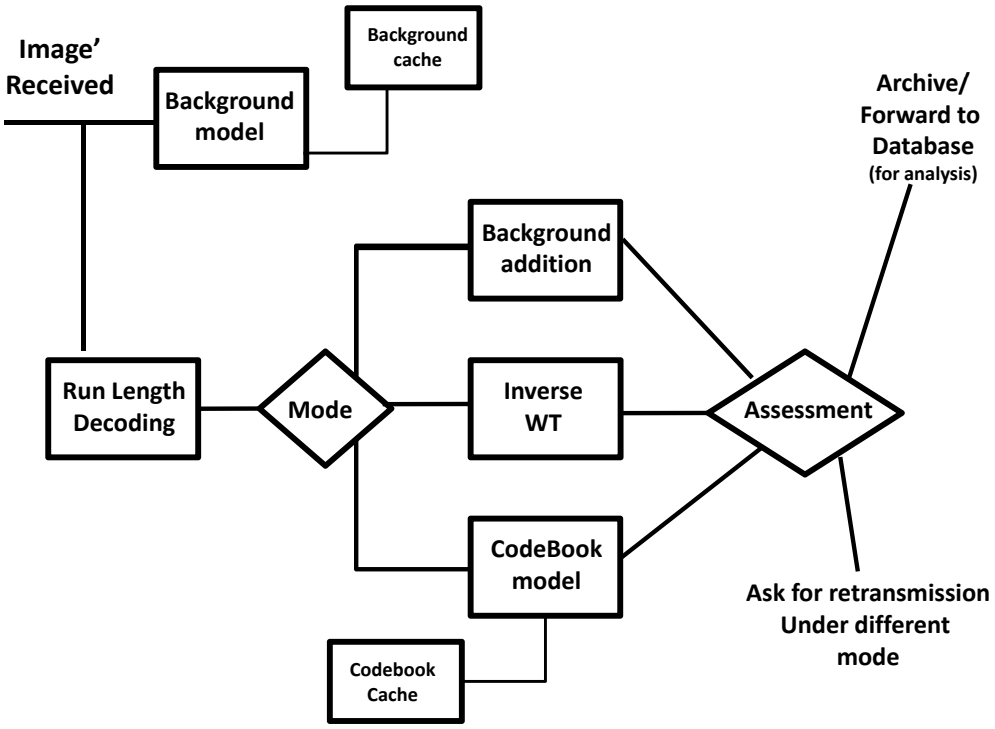

Fig. 8.1.: Decoder design

Then compute the I_{recon} by

$$I_{recon} \quad = \quad I_{fg} + I^B$$

where I_{fg} is the decoded signal.

Once the image is reconstructed, the decoder will run a quality assessment tool described in Chapter 7 (unless it is not required on this transmission). If the quality of the reconstructed image is good, the data will be archived for further processing. If the quality of the reconstructed image is below the quality the application requires, information will be sent using the feedback channel to switch encoding mode to DWT and update the background model. The encoder of the sensor will use this transmission to update its encoder mode.

Decoding Packet Encoded Using Discrete Wavelet Transform (DWT)

If the received packets from the sensors were encoded using DWT, then the Inverse Wavelet Transform (IWT) operation will be executed to reconstruct the original signal from the wavelet coefficients.

The original pixel values can be reconstructed using a multilevel wavelet reconstruction of the bitstream based on the wavelet decomposition structure from the wavelet decomposition step. After reconstruction the quality of the reconstructed image will be assessed (unless it is not required on this transmission) and if the quality is less than the value the application requires, the encoder will be flagged to send more refinement bits (such as to send $LH2$ for an image encoded with 3 levels of wavelet decomposition).

Decoding Packet Encoded Using Codebook

If the mode was codebook, the decoder will use the codebook ID of the neighbor sensor that was used to piece together pieces transmitted by sensor and pieces transmitted by neighbor. For the pieces transmitted by sensor they may have been transmitted by background subtraction, wavelet transform or neither. After piecing together the reconstructed image, the base station will assess the quality of the image (unless it is not required on this transmission).

8.1.2 Block Matching Algorithm (BMA)

It has been widely argued, that a group of sensors performs better in the sensing task than one powerful sensor [32]. In such a sensor network, a group of spatially proximate sensors are very likely to have correlated readings, i.e. due to high density in network topology, sensor observations are highly correlated in the space domain (spatial correlation). Furthermore, the nature of the physical phenomenon constitutes the temporal correlation between each consecutive observation of a sensor node. It is

important to design a good algorithm to exploit this correlation to save transmission power on these resource constrained devices (sensors). If information covering a certain area that's monitored is sent by one of the neighbor sensors, the next sensor monitoring part of that area should take advantage of its neighbor's transmission. The search algorithm will be computationally intensive, so the base station (decoder) will compute the position vectors and transmit this information back to the encoder using the feedback channel.

Exploiting Spatial/Temporal Correlation: Using Block Matching Algorithm

Consider an image divided into small non-overlapping macro blocks (e.g. 16×16). For each block in the first image the algorithm tries to find a block of the same size in the second image that is most similar to the block in the first image within a suitably sized search range (R). Different metrics can be used to measure similarity such as computing the difference between blocks and use cross correlation, squared difference, absolute difference, etc. In our experiment, the metric used for matching the macro blocks is mean absolute difference (MAD), a small MAD implies macro blocks are similar (with some threshold).

$$MAD(A, B) = \frac{1}{m \cdot n} \sum_{p=1}^{m} \sum_{q=1}^{n} [A(p, q) - B(p, q)] \tag{8.1}$$

The function searches in the neighborhood of some given point in the second image by shifting points in the block by the same offset. At each shift, the sum of the distance between the gray values of the two macro blocks is computed. The shift which gives the smallest distance is considered the best match. The search range and how we measure similarity has a great effect in the block matching algorithm, i.e. wider search range will result in the best match but at the expense of computation, and the threshold determines how similar the two macro-blocks are. A fairly low threshold has to be set to get less distortion between the two macro blocks since those blocks who are discovered "matched" by the algorithm will not be encoded

again, rather they will be appended from the previously decoded block from the neighbor's measurement.

The search for a good macroblock match is constrained up to R pixels on all sides of the corresponding macroblock in previous frame from the neighbors sensor. As described the larger the search parameter R the more computationally expensive the process of searching the matched macroblock. So a smart search, such as considering the continuity of position vectors, has to be implemented for efficient processing.

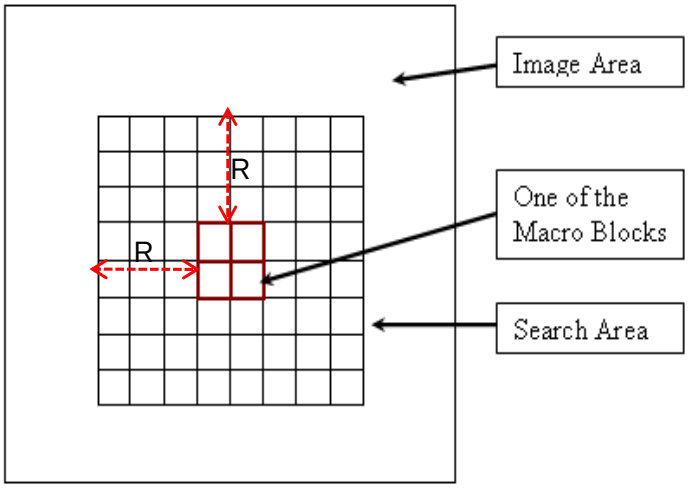

Fig. 8.2.: Block is moved to all vertical, horizontal, left and right displacements in the search area (R from all sides of the macro block) until a match is found with in the given threshold (matching is based on mean absolute difference).

8.1.3 Checking Quality of the Reconstructed Image

The image quality will be assessed using the techniques in Chapter 7. The decoder receive compressed streams that is encoded using either of the encoding techniques described in chapter 6. Once the bitstream is decoded and the image is reconstructed, the quality of the reconstructed image has to be assessed if it meets the quality

Algorithm 5 Block Matching Algorithm (BMA) using exhaustive search with in the search parameter

Input: *mbSize, searchRange, searchIncr, Image, refImage, row, col, thresh*

Output: *codeBk*

1: **for** $i = 1$ to row **do**
2: **for** $j = 1$ to col **do**
3: codeBk$(i, j) = 0$
4: **for** $i = 1$ to $row - mbSize + 1$ **step** $i = i + mbSize$ **do**
5: **for** $j = 1$ to $row - mbSize + 1$ **step** $i = i + mbSize$ **do**
6: FOUND = 0
7: **for** $m = -searchRange$ to $searchRange$ **step** $m = m+searchIncr$ **do**
8: **for** $n = -searchRange$ to $searchRange$ **step** $n = n+searchIncr$ **do**
9: **if** $mbSize \times mbSize$ block determined by coordinate $(i+m, j+n)$ is entirely contained within *refImage* **then**
10: Let *cost= MeanAbsoluteDistance(Block(Image, i,j,mbSize), Block(refImage, i+m,j+n,mbSize)*)
11: **if** cost $\leq$ thresh **then**
12: codeBk$(i, j) = i + m + row \cdot (j + n)$
13: *FOUND=1*
14: break
15: **if** *FOUND = 1* ***then***
16: *break*

required by the application. For example, if the application is for surveillance, a little more lossy is tolerable.

As discussed earlier we will use Reduced-Reference (RR) quality assessment methods in which partial information regarding the 'perfect version' is available. Formally, a side-channel (called an RR channel) exists through which some information regarding the reference can be made available to the QA algorithm. RR QA algorithms use this partial reference information to judge the quality of the reconstructed signal.

Image thumbnail as a side information, as described in Section 7.3.1, the image thumbnail is created after partitioning the image in to square blocks of pixels in which a single mean value representing each block. There is an inverse proportionality between the size of each macroblock and the how close the thumbnail image represent the reference image. A single mean value representing each block will create the thumbnail version of the reference image and this thumbnail version will be sent to the decoder using the side channel. The decoder will reconstruct the image from the bitstreams received from each sensor and create thumbnail version of the reconstructed image using same procedure above. The thumbnail version of the original and reconstructed will be can be used to computer the standard quality assessment tools as MSE or PSNR. As can be seen in Figure 7.3 in Chapter 7, there is a high correlation (almost identical) between reference image and its reconstructed version and their thumbnail version.

Mean and Variance hypothesis test, Since we do not have the reference image at the decoder side to evaluate the quality of the reconstructed image, we have proposed to use both a mean and variance hypothesis test using side information from the encoder. This method is described in Chapter 7.

9. CONCLUSION AND FUTURE WORK

Conclusion:

In this thesis we have constructed a full codec for lightweight encoding for devices with resource constraints like wireless sensor networks, PDA, etc. The codec is designed targeting applications that tolerates a bit more loss of information during source coding than `MPEG 2/4` or `H.264`, like surveillance applications. We also showed the insecurity of wavelet tree shuffling scheme as the only security mechanism in multimedia encryption and propose it as a supplementary security mechanism.

In Chapter 34, we have reviewed selective encryption on wavelet based compression techniques and assessed the security of some of the proposed selective encryption algorithms. Specifically we have assessed the algorithm proposed by Kwon et. al. [5] for selectively encrypting the content of video file for digital rights management. We showed the flaw of the design and suggest that wavelet tree shuffling will not give the desired security if it is used as the only security mechanism.

In Chapter 5, we have provided the overall design of the codec. We also provide the metrics that we used in the subsequent chapters to evaluate the performance of our codec design.

In Chapter 6, we have discussed and provided encoding system in which it can be optimized to the level the application requires. The encoding system will switch between three compression modes (DWT, background subtraction and codebook) for efficient operation. We have used integer based Haar wavelets for efficient operation in resource constrained devices, and simple differencing between a background model representing the static scene of each sensor camera. We have suggested a quantization scheme to encode each pixel during run length encoding of the foreground image. In addition, we have suggested a block matching algorithm to exploit the spatial correlation between proximate sensor reading. Searching of a match in a block matching

algorithm very intensive computation and it is infeasible to implement the algorithm in sensor nodes. Thus, we have switched the traditional encoding order complex encoder simple decoder to simple encoder to complex decoder (assuming the decoder in the base station side has enough computation resources).

In Chapter 7, we have proposed different Reduced-Reference (RR) image quality assessment tools to evaluate the quality of the reconstructed image in the decoder side without having the original image. We have proposed sending the scaled version (mean of each macroblock) of each frame as a side information and scaling the reconstructed image using same procedure to assess quality of the reconstructed image. We have found this method by itself is not sufficient to assess quality and we have added statistical test (Mean and Variance test) to supplement the previous method.

In Chapter 8, We have described the decoding of bitstream encoded using the different source coding techniques proposed in the the encoding system. Most of the decoding is just the reverse operation of the encoding.

Future Work: All our results here are either theoretical analysis (counting clock cycles) and simulations using MatLab. In future work it has to be implemented in sensors and gather real time data for analysis. The block matching algorithm we proposed for exploiting correlated readings between sensors is computationally intensive. Although the Base Station is assumed to have sufficient computational resources, the block matching algorithm has to be developed to be more for efficiency. An exhaustive analysis of the parameter choices should be made for algorithms we have developed to provide more intuition as to what threshold levels should be set for what type of surveillance images and what the necessary significant levels to provide quality assessment.

In this work we only work on the signal processing algorithm and in future work the network protocol has also be studied and designed well to prolong the life time of the network/devise.

LIST OF REFERENCES

LIST OF REFERENCES

[1] "Recommendation for Key Management," *Special Publication 800-57 Part 1, NIST*, 03/2007.

[2] Keylength - Cryptographic Key Length Recommendation. http://www.keylength.com.

[3] R. Cramer and V. Shoup, "A Practical Public Key Cryptosystem Provably Secure against Adaptive Chosen Ciphertext Attack," In *Advances in Cryptology – CRYPTO '98 proceedings*, 1998, pp. 13-25.

[4] B. Furht and D. Kirovski, Eds. *Multimedia Security Handbook*, CRC Press, 2004.

[5] G. Kwon, T. Lee, K. Kim, J.. Jin, and S. Ko, "Multimedia digital right management using selective scrambling for mobile handset," *Computational Intelligence and Security*, LNAI, vol. 3802, pp. 1098-1103, 2005.

[6] W. Li, "Overview of Fine Granularity Scalability in MPEG-4 Video Standard," *IEEE Trans. on Circuits & Systems for Video Technology*, vol.11, no.3, pp. 301-317, March 2001.

[7] A. Massoudi, F. Lefebvre, C. De Vleeschouwer, B. Macq, B. and J. Quisquater, "Overview on selective encryption of image and video: challenges and perspectives," *EURASIP J. Inf. Security*, pp. 1-18, 2008.

[8] Y. Mao and M. Wu, "A joint signal processing and cryptographic approach to multimedia encryption," *IEEE Trans. Image Processing*, 15 (7) (2006), pp. 2061-2075.

[9] R. Norcen and A. Uhl, "Encryption of wavelet-coded imagery using random permutations," in *Proceedings of the IEEE International Conference on Image Processing (ICIP04)*, (Singapore), IEEE Signal Processing Society, Oct. 2004.

[10] M. Podesser, H. Schmidt, and A. Uhl, "Selective bitplane encryption for secure transmission of image data in mobile environments," In *Proceedings of the 5th Nordic Signal Processing Symposium (NORSIG 02)*, 2002.

[11] A. Pommer and A. Uhl, "Selective encryption of wavelet-packet encoded image data: efficiency and security", *Multimedia Systems*, vol. 9, no. 3, pp. 279-287, 2003.

[12] A. Said and W.A. Pearlman, "A new, fast and efficient image codec based on set partitioning in hierarchical trees," In *IEEE Trans. Circuits and Systems for Video Technology*, volume 6(3), pp. 243-250, June 1996.

[13] P. Salama and B. King, "Efficient secure image transmission: compression integrated with encryption," *Proc. SPIE.*, Vol. SPIE-5681, pp. 47-58, 2005

[14] M. Shapiro, "Embedded Image Coding using Zerotrees of Wavelet Coefficients," *IEEE Trans. Signal Processing*, Vol. 41, pp. 3445-3462, 1993.

[15] A. Shamir, "How to share a secret," *Comm of ACM*, vol. 22, no. 11, pp. 612-613, November 1979.

[16] D. Stinson, *Cryptography: theory and practice*, 2^{nd} ed., CRC Press, 2002.

[17] T. Uehara, R. Safavi-Naini, and P. Ogunbona, "Securing wavelet compression with random permutations," in *Proceedings of the 2000 IEEE Pacific Rim Conference on Multimedia*, Sydney, Dec. 2000, pp. 332-335, IEEE Signal Processing Society.

[18] Z. Wang, Alan C. Bovik, Hamid Rahim Sheikh, Eero P. Simoncelli, "Image Quality Assessment: From Error Visibility to Structural Similarity," in *IEEE TRANSACTIONS ON IMAGE PROCESSING* VOL. 13, NO. 4, APRIL 2004

[19] H. R. Sheikh, A. C. Bovik, and L. K. Cormack, "No-Reference Quality Assessment Using Natural Scene Statistics: JPEG2000," in *IEEE Transactions on Image Processing* Vol. 14, No. 12, December 2005.

[20] K. Hasan and K. HaradaII, "Haar Wavelet Based Approach for Image Compression and Quality Assessment of Compressed Image," in *IAENG International Journal of Applied Mathematics*

[21] A. Gersho and R. M. Gray, "Vector Quantization and Signal Compression," Kluwer Academic Publishers, 1991.

[22] M. Nelson, The Data Compression Book, 2nd edition., M&T books,November.1995, As appeared in http://www1.fatbrain.com/asp/bookinfo/bookinfo.asp?theisbn=1558514341

[23] K. Veeraraghavan, D. Peng, and H. Sharif, "Energy efficient multiresolution visual surveillance on wireless sensor networks," in *IEEE International Conference on Electro Information Technology*, Lincoln, NE, 22-25 May 2005, p. 6 pp.

[24] R.C. Gonzalez and R.E. Woods, "Digital Image Processing," Pearson Education, 2003, Chapter 7 - Wavelets and Multiresolution Processing, pp. 349-394.

[25] A. Wang, W. R. Heinzelman, A. Sinha, and A. Chandrakasan, "Energy-scalable protocols for battery-operated microsensor networks," J. VLSI Signal Processing, pp. 223-237, Nov. 2001.

[26] A. Wang, A. Chandrakasan, "Energy-efficient DSPs for wireless sensor networks," in *Signal Processing Magazine, IEEE*, Volume: 19 , Issue: 4

[27] M. Ettus, "System capacity, latency and power consumption in multihop-routed SS-CDMA wireless networks," in *Proc. Radio and Wireless Conference (RAWCON 98)*, Aug. 1998, pp. 55-58.

[28] *TMS320C67x CPU and Instruction Set Reference Guide, TMS320C6000 DSP Platform, Texas Instruments*, Oct 2000, pp. 4.1-4.89, Literature Number: SPRU189F.

[29] L. Liu, Z. Li, E. J. Delp, "Efficient and Low-Complexity Surveillance Video Compression Using Backward Channel Aware Wyner-Ziv Video Coding," In *IEEE Trans. on Circuits and Systems for Video Technology*, volume 19(4), pp. 453-465, April 2009.

[30] M . Srivastava, "Energy efficient wireless systems," in*Submitted for publication in DIMACS Summer School on Foundations of Wireless Networks and Applications*, August 2000 .

[31] G.J. Pottie, W.J. Kaiser, "Wireless Integrated Network Sensors," in *Comm. ACM*, vol. 43, no. 5, pp. 51-58, May 2000.

[32] S. K. Jayaweera, R. Viswanathan, "Distributed Signal Processing in Wireless Sensor Networks," in *IEEE Communication Letters*, Vol. 9, pp. 769-771, Sept. 2005.

[33] M. C. Vuran, O. B. Akan, I. F. Akyildiz, "Spatio-temporal correlation: theory and applications for wireless sensor networks," As appeared in http://www.elsevier.com/locate/comnet

[34] B. Girod, A. Aaron, S. Rane, D. Rebollo-Monedero, "Distributed video coding," Proc. IEEE 93 (1) (2005) 7183.

[35] M. Tahir and R. Farrell,"Optimal communication-computation tradeoff for wireless multimedia sensor network lifetime maximization," in *Proceedings of the 2009 IEEE conference on Wireless Communications & Networking Conference*, isbn = 978-1-4244-2947-9, 2009, 2514–2519.

[36] V. Raghunathan, C. Schurgers, S. Park, and M. B. Srivastava, "Energy Aware Wireless Sensor Networks," in *IEEE Signal Processing Magazine*, 19(2):4050, 2002.

[37] D. Estrin and R. Govindan, "Next century challenges: scalable coordination in sensor networks," in *Proc. Mobicom*, pp. 263-270, 1999.

[38] W. Heinzelman, A. Chandrakasan, and H. Balakrishnan, "Energyefficient communication protocol for wireless sensor networks," in *Proc. Hawaii Intl. Conf. on System Sciences*, Hawaii, 2000.

[39] C. Schurgers and M. Srivastava, "Energy efficient routing in sensor networks," in Proc. Milcom, 2001.

[40] C. Wren, A. Azarhayejani, T. Darrell, and A.P. Pentland, "Pfinder: real-time tracking of the human body," in *IEEE Trans. on Patfern Anal. and Machine Infell.*, vol. 19, no. 7, pp. 78g785, 1997.

[41] B.P.L. Lo and S.A. Velastin, "Automatic congestion detection system for underground platforms," in *Proc.ISIMP2001*, pp. 158-161, May2001.

[42] R. Cucchiara, C. Grana, M. Piccardi, and A. Prati, "Detecting moving objects, ghosts, and shadows in video streams," in *IEEE Tran. on Pattern Anal. and Machine Intell.*, vol. 25, no. 10, pp. 1337-1442,2003

[43] C. Stauffer and W.E.L. Grimson, "Adaptive background mixture models for real-time tracking," in *Proc. IEEE CVPR 1999*, pp. 246-252, June 1999.

[44] S. G. Mallat, "A Theory for Multiresolution Signal Decomposition: A Wavelet Representation," in *IEEE Transactions on Pattern Analysis and Machine Intelligence*, Vol 11, No. 7, July 1989.

[45] E. J. Stollnitz, T. D. DeRose, D. H. Salesin, "Wavelets for Computer Graphics: A Primer Part I," in *IEEE Computer Graphics and Applications*, 15, May 1995.

[46] J. S. Walker, *A Premier on Wavelets and Their Scientific Applications*. Chapman & Hall, 2008.

[47] A. Papoulis, S. U. Pillai, *Probability, Random Variables and Stochastic Processes*. Mc Graw Hill, Fourth Edition.

[48] A. Elgammal, R. Duraiswami, D. Harwood, and L. S. Davis"Background and foreground modeling using nonparametric kernel density estimation for visual surveillance," in *Proceedings of the IEEE*, 90(7):1151-1163, July 2002.

[49] J. Rymel, J. Renno, D. Greenhill, J. Orwell, G.A. Jones, "Adaptive eigenbackgrounds for object detection," in *International Conference on Image Processing, ICIP '04*, Oct. 2004, Vol. 3, 24-27 Oct.

[50] Y. Yu, V. K. Prassana, B. Krishnamachari, V.K Kumar, "Information Processing and Routing in Wireless Sensor Networks," World Scientific Publishing Co. Pte. Ltd, 2006.

[51] I.F Akyildiz, W. SU, Y. Sankarasubramaniam, E. Cayirci, "Wireless Sensor Networks: a survey," in *Computer Networks*, 38, pp. 393-422, 2002.

[52] A. Perrig, J. Stankovic, D. Wagner, "Security in Wireless Sensor Networks"

[53] W. Stallings, L. Brown, *Computer Security: Principles and Practice*. Pearson Education. Inc, 2008.

[54] B. Fyrht, D. Kirovski, *Multimedia Security Handbook*. CRC Press LLC, December 2004.

[55] H. Kiya, D. Imaizumi, and O. Watanabe, "Partial-scrambling of images encoded using JPEG2000 without generating marker codes," in *Proc. IEEE Int. Conference on Image Processing (ICIP2003)*, volume 3, pages 205208, 2003.

[56] C. Shi and B. Bhargava, "Light-weight MPEG video encryption algorithm," in *Proc. Int. Conference on Multimedia (Multimedia 98), Shaping the Future*, pages 5561, 1998.

[57] B. Bhargava, C. Shi, and S.y Wang, "MPEG video encryption algorithms. Multimedia Tools and Applications," 24(1):5779, 2004.

[58] M.S Kankanhalli and T. Guan, "Compressed-domain scrambler/descrambler for digital video," in *IEEE Trans. Consumer Eletronics*, 48(2):356365, 2002.

[59] W. Zeng and S. Lei, "Efficient frequency domain video scrambling for content access control," in *Proc. 7th ACM Int. Conference on Multimedia*, pages 285294, 1999.

[60] A. Uhl and A. Pommer, *Image and Video Encryption: From Digital Rights Management to Secured Personal Communication*. Boston: Springer, 2005.

[61] S. Jalal, B. King, "An Anonymous Authentication Protocol: Acieving Provacy with Trust," MSc Thesis, Purdue University, Indianapolis.

[62] A. Eskicioglu and E. J. Delp, "An Integrated Approach To Encrypting Scalable Video," in *Proceedings of the IEEE International Conference on Multimedia and Expo*, August 26-29, 2002, Lausanne, Switzerland

[63] R. B. Wolfgang and E. J. Delp, "Overview of Image Security Techniques with Applications in Multimedia Systems," in *Proceedings of the SPIE Conference on Multimedia Networks: Security, Displays, Terminals, and Gatweys*, Vol. 3228, November 2-5, 1997, Dallas, Texas, pp. 297-308

[64] M. Eskicioglu, J. Town, and E. J. Delp, "Security of Digital Entertainment Content from Creation to Consumption," in *Proceedings of the SPIE Conference on Applications of Digital Image Processing XXIV*, Vol. 4472, San Diego, July 2001, pp. 187-211

[65] M. Eskicioglu and E. J. Delp, "An Overview of Multimedia Content Protection in Consumer Electronics Devices," in *Proceedings of the SPIE International Conference on Security and Watermarking of Multimedia Contents II*, Vol. 3971, January 23 - 28, 2000, San Jose, CA.

[66] R. B. Wolfgang and E. J. Delp, "Overview of Image Security Techniques with Applications in Multimedia Systems," in *Proceedings of the SPIE Conference on Multimedia Networks: Security, Displays, Terminals, and Gatweys*, Vol. 3228, November 2-5, 1997, Dallas, Texas, pp. 297-308.

[67] Y. Benezeth, P. Jodoin, B. Emile, H. Laurent, and C. Rosenberger, "Review and evaluation of commonly-implemented background subtraction algorithms," in 19th International Conference on Pattern Recognition (ICPR), Tampa, Florida, December 2008, pp. 14.

[68] A. Nasipuri and K. Li., "A directionality based location discovery scheme for wireless sensor networks," in *1st ACM Intl Workshop on Wireless Sensor Networks and Applications (WSNA02)*, pages 105111, Atlanta, GA, Sept. 2002.

[69] C. Valens, As appeared in http://pagesperso-orange.fr/polyvalens/clemens/ezw/ezw.html, 1999

[70] As appeared in http://www.keylength.com/

[71] W. Zeng and S. Lei, "Efficient frequency domain selective scrambling of digital video," *IEEE Transactions onMultimedia*, vol. 5, no. 1, pp. 118-129, 2003.

[72] A. Massoudi, F. Lefebvre, C. De Vleeschouwer, B. Macq, and J.-J. Quisquater, "Overview on Selective Encryption of Image and Video: Challenges and Perspectives," in *Hindawi Publishing Corporation, EURASIP Journal on Information Security Volume 2008*, Article ID 179290, doi:10.1155/2008/179290.

[73] *Image & Video Quality Assessment at LIVE(Laboratory for Image & Video Engineering)* As appeared in http://live.ece.utexas.edu/research/quality/intro.htm,